2014-02-01

On Chip Preconcentration and Labeling of Protein Biomarkers Using Monolithic Columns, Device Fabrication, Optimization, and Automation

Rui Yang
Brigham Young University - Provo

On Chip Preconcentration and Labeling of Protein Biomarkers Using Monolithic Columns: Device Fabrication, Optimization, and Automation

Rui Yang

A thesis submitted to the faculty of
Brigham Young University
in partial fulfillment of the requirements for the degree of

Master of Science

Adam T. Woolley, Chair
Jaron C. Hansen
John T. Prince

Department of Chemistry and Biochemistry

Brigham Young University

February 2014

ABSTRACT

On Chip Preconcentration and Labeling of Protein Biomarkers
Using Monolithic Columns: Device Fabrication,
Optimization, and Automation

Rui Yang
Department of Chemistry and Biochemistry, BYU
Master of Science

Detection of disease specific biomarkers is of great importance in diagnosis and treatment of diseases. Modern bioanalytical techniques, such as liquid chromatography with mass spectrometry (LC-MS), have the ability to identify biomarkers, but their cost and scalability are two main drawbacks. Enzyme-linked immunosorbent assay (ELISA) is another potential tool, but it works best for proteins, rather than peptide biomarkers. Recently, microfluidics has emerged as a promising technique due to its small fluid volume consumption, rapidness, low fabrication cost, portability and versatility. Therefore, it shows prominent potential in the analysis of disease specific biomarkers.

In this thesis, microfluidic systems that integrate monolith columns for preconcentration and on-chip labeling are developed to analyze several protein biomarkers. I have successfully fabricated cyclic olefin copolymer (COC) microfluidic devices with standard micromachining techniques. Monoliths are prepared *in situ* in microchannels via photopolymerization, and the physical properties of monoliths are optimized by varying the composition and concentration of monomers to achieve better flow and extraction. On-chip labeling of protein biomarkers is achieved by driving solution through the monolith using voltage and incubating fluorescent dye with protein retained in the monolith. Subsequently, the labeled proteins are eluted by applying voltages to reservoirs on the microdevice and detected by laser-induced fluorescence. Finally, automation of on-chip preconcentration and labeling is successfully demonstrated.

Keywords: Microfluidics, Solid-phase extraction, Monolith, Preconcentration, On-chip labeling

ACKNOWLEDGEMENTS

I have enjoyed and appreciated the time I spent in our research group. I am fortunate to have the opportunity to working with a number of outstanding professors, who have had an invaluable impact on me both as a scientist and a person.

First and foremost, I would like to thank my advisor and committee chair, Dr. Adam T. Woolley, for his understanding, time, encouragement and most importantly, his scientific guidance during the past few years. His passion and optimism inspired me when I encountered bottlenecks; his strong work ethic taught me how to become a scientist; his mentoring provided me with profound knowledge and experience, which are invaluable in all my endeavors.

I also would like to thank my graduate committee members, Dr. Jaron C. Hansen and Dr. John T. Prince, for their valuable ideas and suggestions. I also thank Dr. Steven R. Goates for his help during the past two years.

In addition to my professors, I am grateful for the opportunity to work with a number of outstanding post-docs and students in our group. I would like to thank Dr. Ming Yu, Dr. Pamela Nge, Jayson Pagaduan and Chad Rogers for their help in all aspects of my project.

Finally, I would like to thank my family members, Shulin Yang, Xiaoning Hu, Guilan Yang, and Yuying Guo, for their love, devotion, education, and encouragement. Special thanks to my husband, Baiyu Huang, for his unwavering love and support. I couldn't have accomplished anything without him.

Table of Contents

List of Tables

List of Figures

CHAPTER 1

INTRODUCTION

1.1 Motivation

A biomarker, or biological marker, is a substance whose presence indicates the existence of a certain biological condition. A disease-specific biomarker can be a molecule either produced by infected cells or a specific chemical produced by the human body in response to the disease.[1] Therefore, detection of disease-specific biomarkers is of great importance in the diagnosis, monitoring and treatment of diseases, such as various types of cancers[2-7] and pregnancy complications.[8, 9] Significant research effort has been devoted to developing efficient and effective detection for disease-specific biomarkers. To date, approximately 115,000 papers have been published on the topic of biomarker-related detection.

Despite outstanding progress achieved to date, effective analytical techniques for disease biomarkers, pathogenic bacteria and virus detection remain a significant challenge.[10] Modern bioanalytical techniques, such as liquid chromatography with mass spectrometry (LC-MS), has the ability to identify biomarkers, but the cost and scalability are two main drawbacks.[11] Enzyme-linked immunosorbent assay (ELISA) is another powerful technique to measure serum biomarkers, but it works best for protein rather than peptide biomarkers.[12] On the other hand, microfluidics, especially integrated microfluidic devices, have emerged as a promising technique due to their small fluid volume consumption, rapidness, low fabrication cost, and portability.[13-17] Furthermore, the miniaturization of traditional electrophoretic analysis can realize the automation and parallelization of tests with reduced sample amount, operation time and cost.[18, 19]

Finally, human error and contamination can be potentially reduced by multifunctional integration of sample preparation, detection, and data processing on a single microfluidic device.[20]

1.2 Microfluidics

Microfluidics consists of microfabricated structures to precisely control fluids geometrically constrained to a small size scale, typically between 1 μm and 1 mm. It integrates aspects of many different scientific areas, including chemistry, physics, engineering, and biology to achieve fluidic sampling, control, monitoring, transport, mixing, reaction, incubation and analysis. Since most biological analyses and chemical reactions involve fluid transport, microfluidics is of great significance. As a result, microfluidics has been heavily used in a wide range of applications, including inkjet printing, biological analysis, biochemical detection, chemical synthesis, biomedicine, and drug delivery.

1.2.1 Advantages of microfluidics

Compared to bulk solution chemical and biological analysis, microfluidics offers several advantages.[21] First, due to the small size scale, the diffusion distance for reactants to interact is very short. Thus, for diffusion-limited mixing processes, such as ELISA, the reaction time is much shorter in miniaturized devices.[15] In addition, smaller device dimensions lead to reduced amounts of sample and reagents required for chemical or biological analysis. Another advantage associated with small dimensions is fast heat dissipation. In microchannels, Joule heat dissipation is more effective, and therefore higher voltages can be applied in electrically driven methods to improve separation efficiency. Second, miniaturized devices offer potential for high-throughput analysis. For example, a 384-lane capillary array electrophoresis device was developed on a 200

mm diameter glass substrate and utilized for massively parallel genetic analysis.[22] Furthermore, miniaturized devices offer portability, which enables on-site analysis and point of care diagnoses.

1.2.2 Microchip capillary electrophoresis

Capillary electrophoresis (CE) employs small inner diameter (20-100 μm) capillaries to achieve high efficiency separations under the influence of an electric field. Pioneering work was done by Jorgenson et al.,[23] who applied a voltage of up to 30 kV to Pyrex glass open tubular capillaries with a 75 μm inner diameter and transferred zone electrophoresis into the capillary format. The employment of a capillary solved some common problems with conventional electrophoresis. For example, the surface area to volume ratio is greatly enhanced in a capillary, which eliminates overheating caused by voltage applied. The resulting high efficiency separation abilities attracted growing interest to further develop this technique. To date, more than 58,000 papers have been published on CE.

In electrophoresis, sample ions move under the influence of an applied voltage. The separation of ions is based on differences in electrophoretic mobility. If band broadening is limited to diffusion, the number of theoretical plates in CE can be calculated using the following equation:

$$N = \frac{\mu_e V}{2D} \tag{1.1}$$

where μ_e is the electrophoretic mobility of the analyte in the separation medium, V is the applied voltage and D is the diffusion coefficient of the analyte. Analytes migrate along the capillary under high voltage and form zones due to differences in their electrophoretic mobilities.

When voltage is applied to the solution in a capillary or microchannel, in many cases electrophoretic movement is not the only driving force in the system. When the inner wall is

charged due to ionization of surface groups or adsorption of ions from the buffer, electroosmotic flow (EOF) is observed. With fused silica, silanol groups on the inner wall are deprotonated to form negatively charged silanoate groups when the pH of the electrolyte solution is above three. These silanoate groups attract cations from the electrolyte solution and form a fixed layer of positive charges at the capillary wall. However, the positive charge in the fixed layer is not sufficient to neutralize all the negative charge, so a second, more loosely bound layer of cations is attracted next to the fixed layer. This second layer is called the mobile layer since it is not bound as tightly as the fixed layer. There is an electrical imbalance associated with the potential difference across these layers, called the zeta potential, ζ. When a voltage is applied along the capillary, the mobile layer is pulled toward the negatively charged cathode. Since the cations are solvated, the bulk buffer solution is dragged by the cations, resulting in EOF. The EOF mobility (μ_{EOF}) is defined as

$$\mu_{EOF} = \varepsilon\zeta / \eta \tag{1.2}$$

where ε is the applied electric field in V/cm, and η is the viscosity of the electrolyte solution.

When considering both electrophoresis and EOF, the theoretical plate number is given by

$$N = \frac{(\mu_e + \mu_{EOF})V}{2D} \tag{1.3}$$

It is important to note that N is proportional to the voltage applied, rather than the length of the capillary, so miniaturized separation channels can still have high separation efficiency. Therefore, microchip CE offers shorter analysis time than traditional CE, with potential for comparable performance. Therefore, microchip CE has been widely used in the separation of DNA,[24, 25] peptides,[26] and proteins.[27, 28]

1.2.3 Integration in microfluidic devices

Although many microfluidic devices have been developed, they are generally considered as "proof of concept" systems and only suitable for samples with low complexity. Applications to actual biological mixtures, which consist of many components with wide concentration ranges, is still under development. Due to the small dimensions of microfluidic platforms, resolving power and peak capacity, which are the two critical parameters for mixture separation, are limited by the separation path. In addition, microfluidic devices often possess short optical detection path, so improvement of detection limits is also needed.

One way to overcome these limitations is by integrating multiple functions onto a single chip. Many processes, such as sample extraction, purification, on-chip labeling and separation can be integrated within a single chip by well-developed photolithography techniques and the development of low-cost plastic materials. For example, samples can be preconcentrated and separated by integrating solid phase extraction (SPE),[29, 30 31] or ion-permeable membranes,[32, 33] with subsequent microchip CE separation. In addition, multi-dimensional separations can be realized on a single device to improve peak capacity, as summarized by Maltezos et al.[34] Furthermore, many of the functions on a microchip are controlled by applying voltage, offering potential for a fully automated platform known as a micro-total-analysis system (μ-TAS) or lab-on-a-chip.

1.3 On-chip sample preparation

One of the most difficult steps in microfluidic integration is sample preparation.[35] Among various sample preparation techniques, SPE is widely used in sample extraction, preconcentration, and purification.[36] Affinity and reversed-phase are two common columns in

SPE. The former has been used to extract or enrich bio-recognizable substances such as cancer biomarkers or PCR products,[30, 37, 38] while the latter is more suitable for extraction of non-polar to moderately polar compounds.[39]

1.3.1 Affinity columns

An affinity column has affinity elements immobilized on a chromatographic column. In affinity columns, affinity elements bind with a specific type of compound, biomedical species, or group of species. Antibody-antigen interaction is one basis of affinity extraction, with antibody immobilized on the column.[40] After sample is introduced, the specific analyte is bound to the antibody on the column while other mixture components are eluted from the column by the mobile phase. Thus, the bound component is separated from the mixture and then eluted from the column by decreasing the affinity between the analyte and the antibody, which is done by changing the pH or ionic strength of the mobile phase,[40] or using a gradient elution technique.[41] Compared to SPE, affinity columns offer high specificity, a significant degree of purification, and good reproducibility.

Affinity columns have been used widely in microfluidic analysis. In 2001, Harrison et al.[42] reported a microchip packed with protein A-coated microspheres for selective clean up and preconcentration of theophylline. Later, Wang et al.[43] reported affinity monolithic columns immobilized with zirconium ions for selective enrichment of phosphopeptides. Peoples et al.[44] demonstrated a direct capture immunoaffinity separation for C-reactive protein (CRP) using a capillary-based microfluidic device. In their study, monoclonal anti-CRP was attached to 5.0 μm streptavidin-coated silica beads to make the solid support for separation columns. Recently, the Woolley group[45] integrated affinity monoliths for on-line protein extraction and preconcentration with CE on poly(methyl methacrylate) microchips. In their study, anti-fluorescein isothiocyanate

(FITC) was immobilized on a monolith to selectively extract FITC-tagged proteins with a 92% elution efficiency. Biotinylated PCR product extraction was also reported by Njoroge et al.[37] PCR products were separated using a streptavidin-modified bed and analyzed by microchip CE.

1.3.2 Packed beads

Beads have been widely used in analytical chemistry for more than three decades. For example, chromatography columns have been packed with small particles to increase the surface to volume ratio and improve separation efficiency. In addition, many kinds of beads are commercially available and their properties are well documented. As a result, beads have been adopted in microchips for SPE.

To increase the surface to volume ratio in microchannels, it is necessary to immobilize the beads within the channel so they are not flushed out when the device is in operation. Currently, several ways have been used to place the beads within a microfluidic device. First, a frit can be fabricated in the microchannel. For example, a sol-gel structure was prepared to retain silica particles for on-chip DNA purification.[46] Alternatively, Harrison et al.[47] used a two weir design to trap silica beads in the reaction chamber, and Andersson et al.[48] demonstrated that a series of pillars could constrain beads placed in a chip. Similarly, Sato et al.[49] demonstrated a "dam" design to constrain beads by constricting the height of the column from 100 μm to 10 μm. In this way, beads can be packed relatively easily and can be modified to have various surface chemistries amenable to analytical operations, such as attaching antibodies.

Fritless designs have also been developed for packing beads. Ceriotti et al.[50] used a tapered channel to trap beads within a microfluidic system. Particles with a diameter of 3 μm were retained and packed without using a frit structure. Another approach was introduced by Andersson et al.,[51] which allowed beads to be patterned on silica surfaces without the need for

packing in a chamber on a device. In their study, the surface of the microchannel was modified using a microcontact printing method. Beads were then placed within the microfluidic chip and self-assembled as a monolayer in the chip. Functionalized beads have also been assembled on surfaces using hydrophobic/hydrophilic interactions,[52] and oligonucleotides.[53] Another interesting approach to achieve a self-assembled bead system enabling selective release was introduced by Malmstadt et al.[54] This approach involved using beads modified with temperature sensitive poly(N-isopropylacrylamide), which underwent a hydrophilic to hydrophobic phase transition at temperatures higher than the lower critical solution temperature. The beads were collected in the channel at an elevated temperature where they aggregated on the sides of the channel, and were released from the channel to be detected at lower temperature.

Beads can be fabricated in a variety of ways using several different materials with various useful functionalities. As a result, they are widely used in microfluidics, as summarized in recent reviews.[55-58] However, packed columns have some limitations associated with packing procedures, surface modification, and design constrains, which increase the complexity of the overall microchip fabrication.

1.3.3 Monolithic columns

Monolithic columns are seeing increased usage in microfluidics due to their easy preparation, no need for retaining structures, and tunable porosity and surface area.[59] A comparison of monoliths and packed beads is shown in Table 1.1.

The first use of a monolith in a chip for SPE was reported by Svec et al.[60] Porous polymer monoliths with two different surface chemistries, hydrophobic and hydrophilic, were obtained using poly(butyl methacrylate-*co*-ethylene dimethacrylate) and poly(2-hydroxyethyl methacrylate-*co*-[2-(methacryloyloxy)ethyl]-trimethylammonium, respectively. An enrichment

of the tetrapeptide Phe-Gly-Phe-Gly up to 1000 fold was reported.[61] Similarly, Tan et al.[62] developed a device with multiple hydrophobic monoliths fabricated within channels on a cyclic olefin copolymer (COC) chip, in which imipramine was extracted from human urine. Capillary electrochromatography is another application of monoliths that has been applied to chip based assays. Shediac et al.[63] made UV initiated acrylate-based porous polymer monoliths as stationary phases for chip electrochromatography of amino acids and peptides. In addition to SPE applications, monoliths have also been utilized in other sample preparations. In a study by Rohr et al.,[64] a photoinitiated monolith was used to assist in mixing of two fluorescent fluids. In another study by Yu et al.,[65] a thermally responsive monomer was adapted into the monolith and the monolith acted as a valve under temperature variation.

Table 1.1 Comparison of monoliths and packed beads for microchips

	Monolithic Phase	Packed beads
Advantages	• Ease of in-situ preparation • Control of pore properties • High flow rate • Flexible modification • Molded into any shape • No frit • Relatively biocompatible	• High surface area • Higher column efficiencies • Small particle size • High operating pressures • Diverse column chemistry • Validated applications • Commercially available
Disadvantages	• Lower surface area • Lower column efficiency • Lower column to column reproducibility	• High back pressure • Frit needed • Difficult to pack into microchannels

Although monoliths possess a number of advantages compared to other on-chip sample preparation media, some disadvantages and limitations are inevitable. One of the drawbacks of monoliths is that in order to produce multiple functionalities within a single device, different

polymers are required. This can be addressed by in situ surface modification of monoliths through photografting,[66] but that raises complexity. In addition, many polymeric monoliths are reported to swell in organic solvents, which reduces their stability. Furthermore, micropores are usually observed, which has a detrimental effect on the separation efficiency and peak symmetry in the column. Finally, technical expertise is required to produce monoliths, and batch-to-batch reproducibility can be a concern.

1.4 Preparation of polymeric monoliths

The preparation of a polymer based monolithic column in a microchannel is relatively simple. Briefly, a mixture of monomers, cross-linker and initiator, as well as porogenic solvents, is loaded into a microchannel. Then polymerization is initiated by heating the mixture, or by exposing the mixture to UV light. After polymerization, a solvent is delivered into the microchannel under pressure or voltage to rinse the monolith. A variety of polymeric monoliths has been fabricated and investigated,[67] including butyl methacrylate,[68] octyl methacrylate,[69] hexyl methacrylate,[70] and lauryl methacrylate[71] as monomers, and EDMA as a cross-linker. By varying the monomer mixture composition, column properties, such as hydrophobicity, pore size and charge, can be manipulated.

Physical properties, such as surface area and pore size, are critical to the application of monoliths in microfluidics, because interacting sites are on the surface of the monolith and the pores are essential for flow. Therefore, optimization of surface area and pore size is required to achieve better loading capacity and separation efficiency. Key factors that affect the pore properties are temperature in thermally initiated polymerization, exposure time in photoinitiated polymerization, and content and composition of monomer solvent mixtures.

Controlling the polymerization temperature is an effective way of manipulating pore size and surface area. Peters et al.[72] reported different pore size ranges obtained at different polymerization temperatures. A narrow pore size distribution was observed when polymerization was carried out at 70 °C, whereas a very broad pore size distribution was obtained when the polymerization temperature was 130 °C. It was reported that temperature affects nucleation rates, and that the difference in pore size range was induced by the difference in the number of nuclei at different temperatures.

Porogen choice is another variable that can be used to control the pore properties without changing the chemical composition of the polymer. It was reported that solvation of the polymer chains in the reaction medium during the early stage of polymerization was affected by the choice of porogenic solvent.[73] Svec et al.[74] showed that the pore size of a poly(glycidyl methacrylate-*co*-ethylene dimethacrylate) monolith could be varied from 90 nm to 400 nm by using different concentrations of dodecanol (6% vs. 12%). In a study by Irgum et al.,[75] the effect of poly(ethylene glycol) (PEG) dissolved in 2-methoxyethanol on the porous polymer was investigated. It was found that larger pore sizes were obtained by using PEG with higher molecular weight. However, the choice of porogens for the preparation of monoliths still remains more empirical than scientific. Therefore, proven porogen mixtures have been repeatedly used for certain types of monoliths. For example, a mixture of cyclohexanol and dodecanol has been used for methacrylate-based monoliths, and a mixture of toluene with longer chain alcohols has been used for the preparation of monoliths from styrene and divinylbenzene.

The crosslinker also affects the morphology of polymeric monoliths. Previous studies showed that the pore size distribution shifted smaller with increased EDMA concentration.[73] Similar to the situation with porogens, the choice of crosslinker is also empirical, and the number

of commonly used crosslinkers is limited. EDMA is most widely used in the preparation of acrylate based monoliths, while divinylbenzene is typically used for styrenic monomers.

1.5 Detection schemes

1.5.1 Electrochemical detection

In microfluidics, electrochemical detection is achieved by monitoring the resistance of a solution or the current from an electrochemical process, known as conductometry and amperometry, respectively. Electrochemical detection offers advantages well suited for microfluidics, including miniaturization capabilities, low cost, low power requirements, low limit of detection (as low as 10 pM), and high compatibility with advanced micromachining and microfabrication technologies.

In conductivity detection, the conductivity difference between background electrolyte in solution and the analyte is measured,[76] by either direct contact between the detection electrodes and the fluid inside the channel,[77] or by an isolated detection electrode integrated on a microchip.[78] Recent applications of conductivity detection in microfluidics are summarized by Hoffman et al.[79]

1.5.2 Optical detection

Compared to electrochemical detection, optical methods have several advantages. They generally have detection limits as low as 1 pM. In addition, optical detection is usually isolated from the fluid, avoiding fouling and bubble formation. Moreover, optical methods can monitor a wide range of compounds that do absorb the optical wavelength.

Laser-induced fluorescence (LIF) is the most widely used optical detection method in microfluidics due to its low detection limit. In this method, a laser is used to excite fluorescent

molecules from the electronic ground state to an excited state. When the excited molecules return to the ground state, light is emitted with a longer wavelength than the laser. Since many samples do not fluoresce naturally, they need to be derivatized with fluorescent tags.[80] In microfluidic systems, the limit of detection is usually limited by the short optical path. In addition, background emission from sources other than the analyte must be eliminated, including scattered laser light, fluorescence from the buffer and the device, Rayleigh scattering, and Raman scattering.

Although LIF has low limits of detection, it also has some disadvantages. LIF often requires delicate and expensive hardware, which limits its miniaturization and portability in point of care applications. In addition, labeling is required for compounds that do not fluoresce naturally, involving time-consuming derivatization procedures.

1.6 Thesis overview

In this thesis, I report the fabrication and optimization of microfluidic columns for solid phase extraction and on-chip labeling. In Chapter 2, I give an overview of the most widely used materials: silicon, glass, and polymers, followed by an introduction of micromachining techniques for cyclic olefin copolymer devices, including photolithography and hot embossing. In Chapter 3, I present the design, fabrication and optimization of monoliths for off-chip solid phase extraction. Monoliths were prepared by in-situ photopolymerization in microchannels. Different types and concentrations of monomers were employed and evaluated, and retention of several proteins was determined in proof of concept experiments. In Chapter 4, I demonstrate automated on-chip labeling experiments using the monoliths optimized in Chapter 3. Finally, in Chapter 5, I give general conclusions from my work and future directions for this research.

References

1. Nass, S. J.; Moses, H. L., *Cancer biomarkers the promises and challenges of improving detection and treatment*. National Academic Press: Washington D.C., 2007.
2. Giribaldi, G.; Barbero, G.; Mandili, G.; Daniele, L.; Khadjavi, A.; Notarpietro, A.; Ulliers, D.; Prato, M.; Minero, V. G.; Battaglia, A.; Allasia, M.; Bosio, A.; Sapino, A.; Gontero, P.; Frea, B.; Fontana, D.; Destefanis, P., Proteomic identification of reticulocalbin 1 as potential tumor marker in renal cell carcinoma. *J. Proteomics* **2013,** *91*, 385-392.
3. Gomes, I. M.; Arinto, P.; Lopes, C.; Santos, C. R.; Maia, C. J., Steap1 is overexpressed in prostate cancer and prostatic intraepithelial neoplasia lesions, and it is positively associated with gleason score. *Urol. Oncol. Semin. Orig. Invest.* **2014,** *32(1)*, 53.e23-53.e29.
4. McKinley, E. T.; Liu, H.; McDonald, W. H.; Luo, W.; Zhao, P.; Coffey, R. J.; Hanks, S. K.; Manning, H. C., Global phosphotyrosine proteomics identifies PKCδ as a marker of responsiveness to Src inhibition in colorectal cancer. *PLoS One* **2013,** *8* (11), e80207.
5. Oyama, K.; Fushida, S.; Kinoshita, J.; Okamoto, K.; Makino, I.; Nakamura, K.; Hayashi, H.; Inokuchi, M.; Nakagawara, H.; Tajima, H.; Fujita, H.; Takamura, H.; Ninomiya, I.; Kitagawa, H.; Fujimura, T.; Ohta, T., Serum cytokeratin 18 as a biomarker for gastric cancer. *Clin. Exp. Med.* **2013,** *13* (4), 289-295.
6. Wang, C.-H.; Lai, H.-C.; Liou, T.-M.; Hsu, K.-F.; Chou, C.-Y.; Lee, G.-B., A DNA methylation assay for detection of ovarian cancer cells using a HpaII/MspI digestion-based PCR assay in an integrated microfluidic system. *Microfluid. Nanofluid.* **2013,** *15* (5), 575-585.
7. Wang, J.; Sharma, A.; Ghamande, S. A.; Bush, S.; Ferris, D.; Zhi, W.; He, M.; Wang, M.; Wang, X.; Miller, E.; Hopkins, D.; Macfee, M.; Guan, R.; Tang, J.; She, J.-X., Serum protein profile at remission can accurately assess therapeutic outcomes and survival for serous ovarian cancer. *PLoS One* **2013,** *8* (11), e78393.
8. Esplin, S.; Merrell, K.; Goldenberg, R.; Lai, Y. L.; Iams, J. D.; Mercer, B.; Spong, C. Y.; Miodovnik, M.; VanDorsten, P.; Dombrowski, M., Proteomic identification of serum peptides predicting subsequent spontaneous preterm birth. *Am. J. Obstet. Gynecol.* **2011,** *204* (391), e1-8.
9. Graves, S.; Esplin, S., Validation of predictive preterm birth biomarkers obtained by maternal serum proteomics. *Am. J. Obstet. Gynecol.* **2011,** *204* (S46).
10. Wang, J.; Chen, G.; Jiang, H.; Li, Z.; Wang, X., Advances in nano-scaled biosensors for biomedical applications. *Analyst* **2013,** *138* (16), 4427-4435.
11. Ishihama, Y., Proteomic LC-MS systems using nanoscale liquid chromatography with tandem mass spectrometry. *J. Chromatogr., A* **2005,** *1067* (1-2), 73-83.
12. Dalvie, M. A.; Sinanovic, E.; London, L.; Cairncross, E.; Solomon, A.; Adam, H., Cost analysis of ELISA, solid-phase extraction, and solid-phase microextraction for the monitoring of pesticides in water. *Environ. Res.* **2005,** *98* (1), 143-150.

13. Behnam, M. K., G. V.; Khorasani, M.; Marshall, P.; Backhouse, C. J.; Elliott, D. G. , An integrated COMS high voltage supply for lab-on-a-chip systems. *Lab Chip* **2008,** *8* (9), 1524-1529.
14. Benhabib, M. C., T. N.; Stockton, A. M.; Scherer, J. R.; Mathies, R. A, Multichannel capillary electrophoresis microdevice and instrumentation for in situ planetary analysis of organic molecules and biomarkers *Anal. Chem.* **2010,** *82*, 2372-2379.
15. Janasek, D.; Franzke, J.; Manz, A., Scaling and the design of miniaturized chemical-analysis systems. *Nature* **2006,** *442* (7101), 374-80.
16. Jiang, H.; Weng, X.; Li, D., Microfluidic whole-blood immunoassays. *Microfluid. Nanofluid.* **2011,** *10* (5), 941-964.
17. Woolley, A. T.; Mathies, R. A., Ultra-high-speed DNA sequencing using capillary electrophoresis chips *Anal. Chem.* **1995,** *67* (20), 3676-3680.
18. Woolley, A. T.; Mathies., R. A., Ultra-high-speed DNA fragment separations using microfabricated capillary array electrophoresis chips. *Proc. Natl. Acad. Sci. U.S.A* **1994,** *91* (24), 11348-11352.
19. Shi, Y. S., Peter C.; Scherer, J. R.; Wexler, D; Skibola, C.; Smith, M. T.; Mathies, R. A., Radial capillary array electrophoresis microplate and scanner for high-performance nucleic acid analysis *Anal. Chem.* **1999,** *71* (23), 5354-5361.
20. Arora, A. S., Giuseppina; Salieb-Beugelaar, G. B.; Kim, J. Tae; Manz, A.; Latest developments in micro total analysis systems. *Anal. Chem.* **2010,** *82* (12), 4830-4847.
21. Whitesides G., M., The origins and the future of microfluidics. *Nature* **2006,** *442* (7101), 368-73.
22. Emrich, C. A.; Tian, H.; Medintz, I. L.; Mathies, R. A., Microfabricated 384-lane capillary array electrophoresis bioanalyzer for ultrahigh-throughput genetic analysis. *Anal. Chem.* **2002,** *74* (19), 5076-5083.
23. Jorgenson, J. W.; Lukacs, K. D., Zone electrophoresis in open-tubular glass capillaries. *Anal. Chem.* **1981,** *53* (8), 1298-302.
24. Castano-Alvarez, M.; Fernandez-Abedul, M. T.; Costa-Garcia, A., Electroactive intercalators for DNA analysis on microchip electrophoresis. *Electrophoresis* **2007,** *28* (24), 4679-4689.
25. Wan, F.; He, W.; Zhang, J.; Chu, B., Reduced matrix viscosity in DNA sequencing by ce and microchip electrophoresis using a novel thermo-responsive copolymer. *Electrophoresis* **2009,** *30* (14), 2488-2498.
26. Sun, X.; Liu, J.; Lee, M. L., Surface modification of glycidyl-containing poly(methyl methacrylate) microchips using surface-initiated atom-transfer radical polymerization. *Anal. Chem.* **2008,** *80* (3), 856-863.
27. El Rassi, Z., Electrophoretic and electrochromatographic separation of proteins in capillaries: An update covering 2007-2009. *Electrophoresis* **2010,** *31* (1), 174-191.
28. Wu, R.; Wang, Z.; Zhao, W.; Yeung, W. S.-B.; Fung, Y. S., Multi-dimension microchip-capillary electrophoresis device for determination of functional proteins in infant milk formula. *J. Chromatogr. A* **2013,** *1304*, 220-226.

29. Nge, P. N.; Pagaduan, J. V.; Yang, W.; Woolley, A. T., Integrated affinity and electrophoresis systems for multiplexed biomarker analysis. *Methods Mol. Biol.* **2013,** *919*, 189-201.
30. Yang, W.; Yu, M.; Sun, X.; Woolley, A. T., Microdevices integrating affinity columns and capillary electrophoresis for multibiomarker analysis in human serum. *Lab Chip* **2010,** *10* (19), 2527-2533.
31. Svec, F., Less common applications of monoliths: Preconcentration and solid-phase extraction. *J. Chromatogr. B.* **2006,** *841* (1-2), 52-64.
32. Kelly, R. T.; Li, Y.; Woolley, A. T., Phase-changing sacrificial materials for interfacing microfluidics with ion-permeable membranes to create on-chip preconcentrators and electric field gradient focusing microchips. *Anal. Chem.* **2006,** *78* (8), 2565-2570.
33. Nge, P. N.; Yang, W.; Pagaduan, J. V.; Woolley, A. T., Ion-permeable membrane for on-chip preconcentration and separation of cancer marker proteins. *Electrophoresis* **2011,** *32* (10), 1133-1140.
34. Maltezos, G. M.; Scherer, A.; Gomez, A.; Gomez, F. A., Chemical separations in three-dimensional microfluidics. *Biol. Appl. Microfluid.* **2008**, 263-272.
35. Verbarg, J.; Kamgar-Parsi, K.; Shields, A. R.; Howell, P. B.; Ligler, F. S., Spinning magnetic trap for automated microfluidic assay systems. *Lab Chip* **2012,** *12* (10), 1793-1799.
36. Yang, H.; Mudrik, J. M.; Jebrail, M. J.; Wheeler, A. R., A digital microfluidic method for in situ formation of porous polymer monoliths with application to solid-phase extraction. *Anal. Chem.* **2011,** *83* (10), 3824-3830.
37. Njoroge, S. K.; Witek, M. A.; Battle, K. N.; Immethun, V. E.; Hupert, M. L.; Soper, S. A., Integrated continuous flow polymerase chain reaction and micro-capillary electrophoresis system with bioaffinity preconcentration. *Electrophoresis* **2011,** *32* (22), 3221-3232.
38. Nguyen, T.; Pei, R.; Stojanovic, M.; Lin, Q., An aptamer-based microfluidic device for thermally controlled affinity extraction. *Microfluid. Nanofluid.* **2009,** *6* (4), 479-487.
39. Liu, J.; Chen, C.-F.; Tsao, C.-W.; Chang, C.-C.; Chu, C.-C.; De Voe, D. L., Polymer microchips integrating solid-phase extraction and high-performance liquid chromatography using reversed-phase polymethacrylate monoliths. *Anal. Chem.* **2009,** *81* (7), 2545-2554.
40. Qian, W.; Yao, D.; Yu, F.; Xu, B.; Zhou, R.; Bao, X.; Lu, Z., Immobilization of antibodies on ultraflat polystyrene surfaces. *Clin. Chem.* **2000,** *46* (9), 1456-63.
41. Ottow, K. E.; Lund-Olesen, T.; Maury, T. L.; Hansen, M. F.; Hobley, T. J., A magnetic adsorbent-based process for semi-continuous pegylation of proteins. *Biotechnol. J.* **2011,** *6* (4), 396-409.
42. Jemere, A. B.; Oleschuk, R.; Taylor, J.; Harrison, D. J., Microchip-based selective preconcentration using protein A immunoaffinity chromatography. *Micro Total Anal. Syst. 2001, Proc. μ TAS 2001 Symp., 5th* **2001**, 501-502.
43. Wang, H.; Duan, J.; Yu, H.; Zhao, L.; Liang, Y.; Shan, Y.; Zhang, L.; Liang, Z.; Zhang, Y., Monoliths with immobilized zirconium ions for selective enrichment of phosphopeptides. *J. Sep. Sci.* **2011**, 34, 2113-2121.

44. Peoples M. C.; Phillips T. M.; Karnes, H. T., Demonstration of a direct capture immunoaffinity separation for c-reactive protein using a capillary-based microfluidic device. *J. Pharm. Biomed. Anal.* **2008,** *48* (2), 376-82.
45. Sun, X.; Yang, W.; Pan, T.; Woolley, A. T., Affinity monolith-integrated poly(methyl methacrylate) microchips for on-line protein extraction and capillary electrophoresis. *Anal. Chem.* **2008,** *80* (13), 5126-5130.
46. Verpoorte, E., Beads and chips: New recipes for analysis. *Lab Chip* **2003,** *3* (4), 60N-68N.
47. Oleschuk, R. D.; Shultz-Lockyear, L. L.; Ning, Y.; Harrison, D. J., Trapping of bead-based reagents within microfluidic systems. On-chip solid-phase extraction and electrochromatography. *Anal. Chem.* **2000,** *72* (3), 585-590.
48. Andersson, H.; van der Wijngaart, W.; Enoksson, P.; Stemme, G., Micromachined flow-through filter-chamber for chemical reactions on beads. *Sens. Actuators, B* **2000,** *67* (1-2), 203-208.
49. Sato, K.; Tokeshi, M.; Odake, T.; Kimura, H.; Ooi, T.; Nakao, M.; Kitamori, T., Integration of an immunosorbent assay system: Analysis of secretory human immunoglobulin a on polystyrene beads in a microchip. *Anal. Chem.* **2000,** *72* (6), 1144-1147.
50. Ceriotti, L.; de Rooij, N. F.; Verpoorte, E., An integrated fritless column for on-chip capillary electrochromatography with conventional stationary phases. *Anal. Chem.* **2002,** *74* (3), 639-647.
51. Andersson, H.; Jonsson, C.; Moberg, C.; Stemme, G., Patterned self-assembled beads in silicon channels. *Electrophoresis* **2001,** *22* (18), 3876-3882.
52. Huang, T. T.; Geng, T.; Akin, D.; Chang, W.-J.; Sturgis, J.; Bashir, R.; Bhunia, A. K.; Robinson, J. P.; Ladisch, M. R., Micro-assembly of functionalized particulate monolayer on C18-derivatized SiO_2 surfaces. *Biotechnol. Bioeng.* **2003,** *83* (4), 416-427.
53. McNally, H.; Pingle, M.; Lee, S. W.; Guo, D.; Bergstrom, D. E.; Bashir, R., Self-assembly of micro- and nano-scale particles using bio-inspired events. *Appl. Surf. Sci.* **2003,** *214* (1-4), 109-119.
54. Malmstadt, N.; Yager, P.; Hoffman, A. S.; Stayton, P. S., A smart microfluidic affinity chromatography matrix composed of poly(n-isopropylacrylamide)-coated beads. *Anal. Chem.* **2003,** *75* (13), 2943-2949.
55. Gijs, M. A. M.; Lacharme, F.; Lehmann, U., Microfluidic applications of magnetic particles for biological analysis and catalysis. *Chem. Rev.* **2010,** *110* (3), 1518-1563.
56. Lim, C. T.; Zhang, Y., Bead-based microfluidic immunoassays: The next generation. *Biosens. Bioelectron.* **2007,** *22* (7), 1197-1204.
57. Lombardi, D.; Dittrich, P. S., Microdroplets and magnetic beads: Fishing for molecules in nl volumes. *Chimia* **2011,** *65* (12), 978.
58. Wen, J.; Legendre, L. A.; Bienvenue, J. M.; Landers, J. P., Purification of nucleic acids in microfluidic devices. *Anal. Chem.* **2008,** *80* (17), 6472-6479.

59. Woodward, S. D.; Urbanova, I.; Nurok, D.; Svec, F., Separation of peptides and oligonucleotides using a monolithic polymer layer and pressurized planar electrophoresis and electrochromatography. *Anal. Chem.* **2010,** *82* (9), 3445-3448.
60. Peterson, D. S.; Rohr, T.; Svec, F.; Frechet, J. M. J., Enzymatic microreactor-on-a-chip: Protein mapping using trypsin immobilized on porous polymer monoliths molded in channels of microfluidic devices. *Anal. Chem.* **2002,** *74* (16), 4081-4088.
61. Yu, C.; Davey, M. H.; Svec, F.; Frechet, J. M. J., Monolithic porous polymer for on-chip solid-phase extraction and preconcentration prepared by photoinitiated in situ polymerization within a microfluidic device. *Anal. Chem.* **2001,** *73* (21), 5088-5096.
62. Tan, A.; Benetton, S.; Henion, J. D., Chip-based solid-phase extraction pretreatment for direct electrospray mass spectrometry analysis using an array of monolithic columns in a polymeric substrate. *Anal. Chem.* **2003,** *75* (20), 5504-5511.
63. Shediac, R.; Ngola, S. M.; Throckmorton, D. J.; Anex, D. S.; Shepodd, T. J.; Singh, A. K., Reversed-phase electrochromatography of amino acids and peptides using porous polymer monoliths. *J. Chromatogr. A* **2001,** *925* (1-2), 251-263.
64. Rohr, T.; Yu, C.; Davey, M. H.; Svec, F.; Frechet, J. M. J., Porous polymer monoliths: Simple and efficient mixers prepared by direct polymerization in the channels of microfluidic chips. *Electrophoresis* **2001,** *22* (18), 3959-3967.
65. Yu, C.; Mutlu, S.; Selvaganapathy, P.; Mastrangelo, C. H.; Svec, F.; Frechet, J. M. J., Flow control valves for analytical microfluidic chips without mechanical parts based on thermally responsive monolithic polymers. *Anal. Chem.* **2003,** *75* (8), 1958-1961.
66. Rohr, T.; Ogletree, D. F.; Svec, F.; Frechet, J. M. J., Surface functionalization of thermoplastic polymers for the fabrication of microfluidic devices by photoinitiated grafting. *Adv. Funct. Mater.* **2003,** *13* (4), 264-270.
67. Wu, R. a.; Hu, L.; Wang, F.; Ye, M.; Zou, H., Recent development of monolithic stationary phases with emphasis on microscale chromatographic separation. *J. Chromatogr. A* **2008,** *1184* (1-2), 369-392.
68. Yan, W.-Y.; Zhang, Z.-C.; Gao, R.-Y.; Yan, C.; Wang, Q.-S., Short, highly cross-linked, polymer based, monolithic column for capillary electrochromatography. *J. Liq. Chromatogr. Relat. Technol.* **2002,** *25* (19), 2965-2976.
69. Huang, X.; Wang, Q.; Yan, H.; Huang, Y.; Huang, B., Octyl-type monolithic columns of 530 μ m i.D. For capillary liquid chromatography. *J. Chromatogr. A* **2005,** *1062* (2), 183-188.
70. Umemura, T.; Ueki, Y.; Tsunoda, K.-i.; Katakai, A.; Tamada, M.; Haraguchi, H., Preparation and characterization of methacrylate-based semi-micro monoliths for high-throughput bioanalysis. *Anal. Bioanal. Chem.* **2006,** *386* (3), 566-571.
71. Dong, J.; Xie, C.; Tian, R.; Wu, R.; Hu, J.; Zou, H., Capillary electrochromatography with a neutral monolithic column for classification of analytes and determination of basic drugs in human serum. *Electrophoresis* **2005,** *26* (18), 3452-3459.

72. Peters, E. C.; Svec, F.; Frechet, J. M. J.; Viklund, C.; Irgum, K., Control of porous properties and surface chemistry in "molded" porous polymer monoliths prepared by polymerization in the presence of tempo. *Macromolecules* **1999,** *32* (19), 6377-6379.
73. Viklund, C.; Svec, F.; Frechet, J. M. J.; Irgum, K., Monolithic, "molded", porous materials with high flow characteristics for separations, catalysis, or solid-phase chemistry: Control of porous properties during polymerization. *Chem. Mater.* **1996,** *8* (3), 744-50.
74. Svec, F.; Frechet, J. M. J., Kinetic control of pore formation in macroporous polymers. Formation of "molded" porous materials with high flow characteristics for separations or catalysis. *Chem. Mater.* **1995,** *7* (4), 707-15.
75. Courtois, J.; Bystroem, E.; Irgum, K., Novel monolithic materials using poly(ethylene glycol) as porogen for protein separation. *Polymer* **2006,** *47* (8), 2603-2611.
76. Vazquez, M.; Frankenfeld, C.; Coltro Wendell, K. T.; Carrilho, E.; Diamond, D.; Lunte Susan, M., Dual contactless conductivity and amperometric detection on hybrid PDMS/glass electrophoresis microchips. *Analyst* **2010,** *135* (1), 96-103.
77. Solinova, V.; Kasicka, V., Recent applications of conductivity detection in capillary and chip electrophoresis. *J. Sep. Sci.* **2006,** *29* (12), 1743-1762.
78. Baker, C. A.; Duong, C. T.; Grimley, A.; Roper, M. G., Recent advances in microfluidic detection systems. *Bioanalysis* **2009,** *1* (5), 967-975.
79. Hoffmann, W.; Muehlberger, H.; Hwang, W.; Petrova, L.; Mootz, T.; Saumer, M.; Guber, A. E.; Saile, V., Advanced conductivity detection for microfluidics. *ECS Trans.* **2008,** *16* (11), 199-207.
80. Myers, F. B.; Lee, L. P., Innovations in optical microfluidic technologies for point-of-care diagnostics. *Lab Chip* **2008,** *8* (12), 2015-2031.

CHAPTER 2

MICROFLUIDIC CHIP FABRICATION

2.1 Introduction

In microfluidics, short reaction times, laminar flows and capillary effects are unique phenomena in the microscale.[1, 2] Therefore, the surface properties of a material are of great importance since they can result in either unique function or problems that do not occur at the macroscale.[3] As a result, the choice of an appropriate material is important to optimizing the function of a microfluidic device.

A variety of materials have been utilized for the fabrication of microfluidic devices. Among these materials, silicon is popular because of well-established micromachining techniques, as well as its mechanical properties, chemical resistance, well characterized processing techniques and the capability for circuitry integration.[4] Glass has also been widely used in microfluidic devices, especially for capillary electrophoresis, due to its optical transparency and ease of electroosmotic flow.[5] Currently, polymers or plastics are very promising materials for microfluidic devices because of their low manufacturing cost and appropriate properties for performing biochemical analyses.

2.1.1 Silicon

Silicon is opaque in the visible light range. Vertical channel sidewalls can be created in silicon crystals. Silicon has good resistance against organic solvents, high thermal conductivity, and reliable electroosmotic flow. In addition, thin films of metal (i.e., Ti/Pt) can be easily deposited on silicon surfaces, for example, to control the heating of microchannels.[6] Given these

advantages, silicon has been widely used in a number of microfluidic applications.[6-18] For example, Harris et al.[7] reported a silicon microfluidic ultrasonic separator. Similarly, Chen et al.[8] developed a crossflow blood filtration system using silicon nano-filters and reported a maximum plasma selectivity of 97.7%. Luque et al.[10] reported a pneumatically actuated silicon microfluidic valve, and a silicon-based thermal distribution microfluidic sensor was reported by Weiping et al.[11]

Wet etching and dry etching are the two mainstream techniques to form channels on silicon substrates.[3] Since crystalline silicon has a preferential etching direction in wet etching, anisotropic channels are produced when potassium hydroxide (KOH), tetramethyl ammonium hydroxide (TMAH), and ethylene diamine pyrocatechol (EDP) are used as etchants.[4] However, isotropic channels can also be prepared by a technique called "HNA" etching, in which a mixture of hydrofluoric acid (HF), nitric acid (HNO_3) and acetic acid (CH_3COOH) are used to etch. In dry etching, the most commonly used process is reactive ion etching. Ions are excited by radio frequency energy and generate physical and chemical reactions on the exposed area of silicon substrates.[19]

Silicon materials also have some limitations. It should be noted that these etching techniques involve dangerous chemicals (*e.g.,* HF) and therefore require specialized facilities. In addition, thermal bonding requires high temperature and pressure and a clean environment; anodic bonding also requires relatively high temperatures, as well as clean and flat wafer surfaces. Furthermore, silicon is gas impermeable, which makes it less attractive for biological applications that involve living cells.

2.1.2 Glass

Glass has similarities with silicon: resistance to organic solvents, high thermal conductivity and stable electroosmotic flow.[3] In addition, glass is optically transparent and electrically insulating, and rounded channel sidewalls are usually produced after wet etching due to the amorphous nature of glass. Wet etching and thermal bonding are the main techniques to form channels on glass substrates.[20, 21] Typical etchants are HF, or a mixture of HF and HNO_3. Glass materials have been widely used in capillary electrophoresis (CE) because: (1) the direct use of electroosmotic flow offers valve free design and short analysis times;[22] and (2) its high thermal conductivity and reliable electroosmotic flow provide better performance than silicon.[3, 23] For example, Manz et al.[20, 21] integrated CE and sample injection on a planar glass chip. Reschke et al.[24] developed a glass microfluidic device for simultaneous separation and detection of cations and anions with suppressed electroosmotic flow and a single injection point. Recently, Meagher et al.[25] reported microchip CE of DNA following preconcentration at photopatterned gel membranes in a glass microfluidic device. Besides CE, glass has also been used as a microfluidic emitter electrospray ionization source.[26-28] Similar to silicon, glass is not gas permeable, which limit its applications in long-term cell culture.

2.1.3 Polymers and plastics

Polymers are a popular and promising substrate material in microfluidics due to their low fabrication cost and massive production capability.[3, 29-31] Poly(methyl methacrylate) (PMMA), poly(dimethylsiloxane) (PDMS) and cyclic olefin copolymer (COC) are three commonly used types of polymers in microfluidics.

Due to its optical transparency and low cost, PMMA has been used widely in microfluidics. For example, Petersen et al.[32] reported a PMMA device that integrated on-chip

polypropylene membrane extraction with online ultraviolet absorbance and mass spectrometric detection. Jubery et al.[33] demonstrated 10,000-fold pre-concentration of cardiac proteins in a PMMA microfluidic device. Reedy et al.[34] also reported solid phase extraction of DNA from biological samples in a post-based PMMA microdevice. Similarly, Hwang et al.[35] reported a PMMA microfluidic device for on-chip extraction of bacterial DNA. PMMA devices for rapid detection of glucose and methanol were also reported.[36, 37] However, PMMA, like silicon and glass, is not gas permeable. In addition, it swells or dissolves in many organic solvents and has poor resistance to many other chemicals. Therefore, biological and chemical compatibility should be taken into consideration when using PMMA.[3]

Similar to PMMA, a significant advantage of PDMS is its ease of prototype fabrication.[31] In contrast to PMMA, PDMS possesses high elasticity, which is useful in microfluidic pump and valve applications. For example, Quist et al.[38] reported elastomeric microvalves in PDMS devices. In addition, PDMS is gas permeable and cell culture compatible, which is necessary for long-term cell culture on an environment controlled microdevice.[39] As a result, PDMS is broadly utilized in bio-related research, such as cell culture and screening, and biochemical assays. [40, 41] For example, Li et al.[42] developed a PDMS microfluidic system to study the response of endothelial cells to pressure. Kayo et al.[43] reported a PDMS microfluidic device for immunoaffinity separation of mitochondria from cell culture. However, PDMS also has notable limitations.[44] PDMS is incompatible with many organic solvent and not suitable for many quantitative experiments because of the absorption of hydrophobic molecules and biomolecules on channel walls, and water loss due to evaporation through the channel walls.[45] Moreover, for many applications, including monolithic solid phase extraction, surface modification is required.[46]

Table 2.1 Overview of different polymer micro/nanofabrication techniques*

	Casting	Hot embossing	Injection molding
Investment	Low	Moderate	High
Manufacturability	Low	Moderate	High
Cycle time	8-10 hours	1 hour	1 min
Polymer choices	Low	Moderate	Moderate
Mold replication	Good	Good	Good
Reusability of mold	No (photolithography-based molds)	Yes	Yes

*Adapted from Ref. 29

Recently, COC has emerged as a promising material in microfluidics. COC has high transmission in the UV and visible, low self-fluorescence, and is stable in organic solvents such as acetonitrile.[47] In addition, stable monoliths can be formed in COC devices without channel surface modification.[48] Therefore, COC is seeing wide application in microfluidic separations with monoliths. For example, Faure et al.[49] developed a COC microfluidic device with an acrylate monolith for chip electrochromatography. Similarly, Ladner et al. [48] reported photopolymerization of an acrylate monolith in COC and its application in electrochromatography. Nge et al.[50] integrated monolithic solid phase extraction and on-chip labeling on a COC microfluidic device for heat shock protein 90, offering promising potential for automated analysis.

One of the most significant advantages of polymers is their massive production availability, which allows commercialization of lab-on-a-chip technology.[29] Currently, casting, hot embossing and injection molding are the three major techniques for device fabrication with a

mold master. Ahn et al.[29] provided an excellent review summarizing the principles for these three fabrication method, and an overview of these techniques is given in Table 2.1.

COC was chosen for this project due to its optical properties, stability in organic solvents and ease of monolith formation. In this chapter, fabrication methods for COC devices using well-established micromachining techniques are presented. Briefly, a silicon master mold is prepared, followed by replica molding of COC on the master mold via hot embossing. Finally, microchannels are formed by attaching the channel layer to another COC slab via thermal bonding.

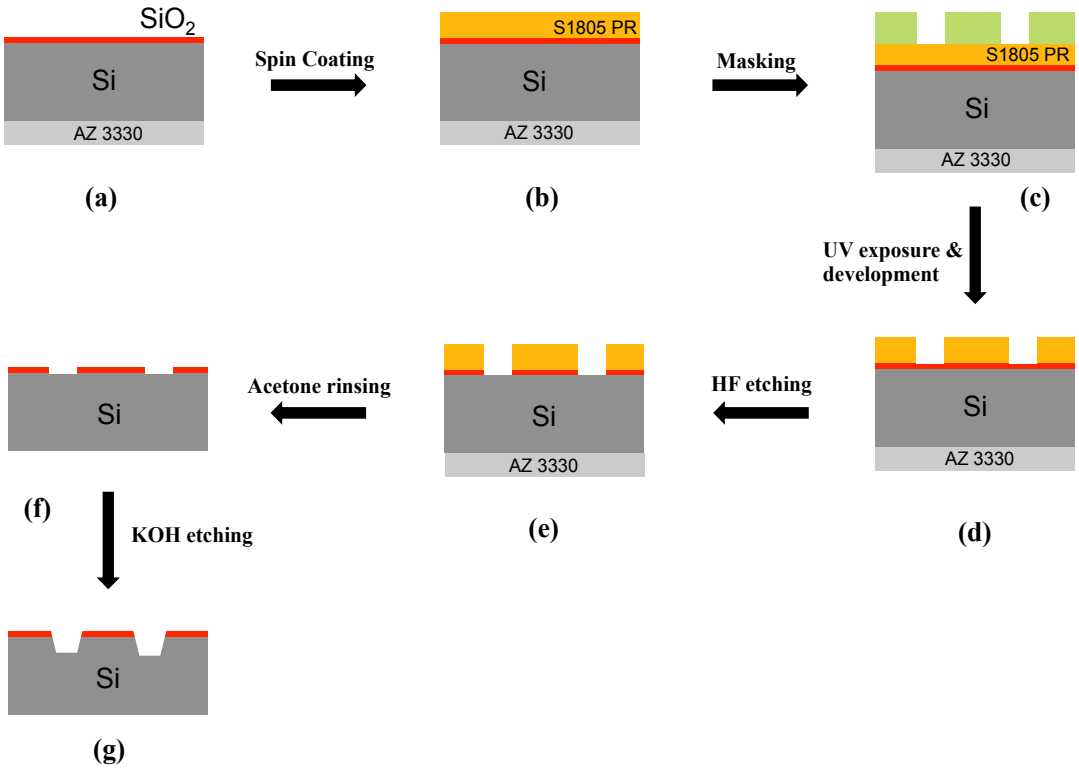

Figure 2.1 Mold fabrication procedures: (a) back side spin-coating of AZ3330, (b) Spin-coating of S1805, (c) masking, (d) UV exposure and development, (e) HF etching of silica layer, (f) removal of remaining S1805, and (g) KOH etching of silicon surface.

2.2 COC device fabrication

2.2.1 Master mold fabrication

The fabrication process of a mold is shown in Figure 2.1. Silicon with a silica layer is used as the mold substrate. After rinsing with acetone and 2-propanol, the wafer is dried in an Ultra-Clean 100 oven (Lab-Line Instruments, Melrose Park, IL) for 15 min at 150 °C. Next, a layer of AZ3330 (AZ Electronic Materials, Branchburg, NJ) is spin-coated at 1000 rpm for 30 seconds to protect the back side (Figure 2.1a). Then the wafer is heated at 110 °C for 2 minutes to remove any residual solvent. Following cooling, a S1805 photoresist layer is spin-coated on the silica surface at 4000 rpm for 60 seconds (Figure 2.1b). After baking at 110 °C for 2 minutes for photoresist dehydration, the mold is cooled to room temperature and then covered with a mask with the desired shape of microchannel (Figure 2.1c). Then the wafer with the mask is exposed to UV light for 10 seconds and developed in MF24A solution for 15 to 20 seconds, depending on the desired channel height (Figure 2.1d). Following rinsing, the exposed silica is etched with HF for 300-400 seconds until the wafer becomes hydrophobic (Figure 2.1e). After HF is rinsed off with deionized water, the unexposed area of S1805 is rinsed off with acetone (Figure 2.1f). Finally, 40 wt% KOH is used to etch the channel shape on the silicon wafer for 45 minutes in a water bath at 70 °C to achieve a channel depth of approximately 20 μm.

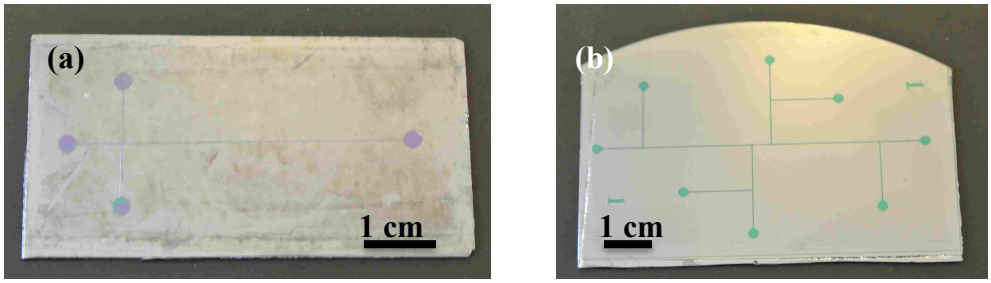

Figure 2.2 Master mold design of COC device: (a) four-reservoir straight channel design, and (b) eight-reservoir design for on-chip preconcentration and labeling.

Two types of master molds have been used in this work (Figure 2.2). The first one is a four-reservoir cross design as shown in Figure 2.2a, which consists of 50 mm and 20 mm channels that intersect. In the preparation and optimization of monoliths (Chapter 3), this master mold was used to produce a 50 mm microchannel device. The second design with eight reservoirs (Figure 2.2b) was used in automation of on-chip preconcentration and labeling, which is discussed in detail in Section 4.2.

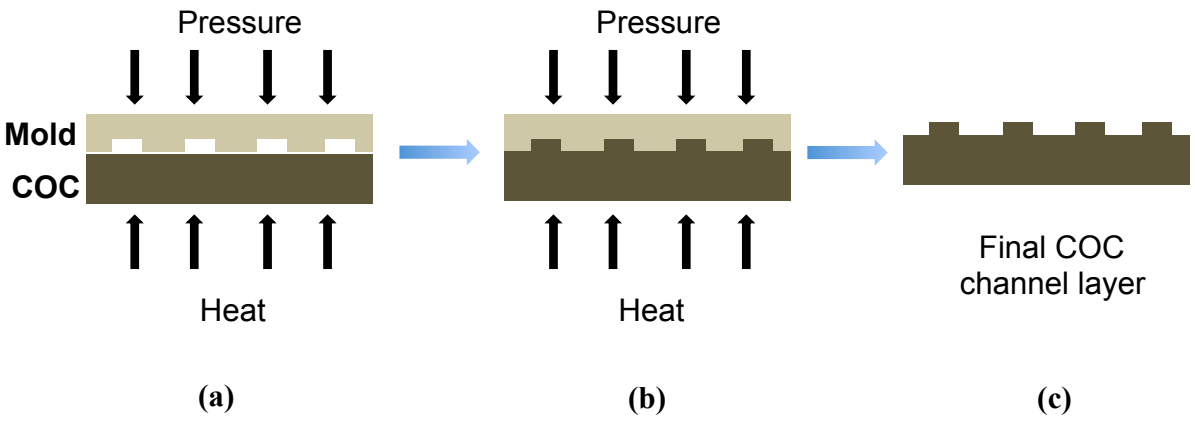

Figure 2.3 Schematic of hot embossing process.

2.2.2 Hot embossing

The microfluidic design was transferred onto COC by hot embossing as shown in Figure 2.3. The master mold obtained in section 2.2.1 and the COC substrate were placed in a muffle oven at 138 °C for 24 minutes. During this process, COC was softened and filled the voids between it and the master mold under pressure. Then the plates were cooled down to release the replicated COC substrate. To form a microchannel, another flat COC slab was attached to the replicated substrate and thermally bonded together in a muffle oven at 110 °C for 28 minutes. After cooling, the COC device was rinsed with isopropyl alcohol to clean the surface of microchannels. The morphology of the microchannels was determined by imaging using a Nikon

Eclipse TE30 inverted microscope with a CCD camera (Coolsnap HQ, Roper Scientific, Sarasota, FL).

2.3 COC device characterization

The fabrication procedure described in section 2.2.2 produced COC devices with microchannels having widths and depths matching those of the master mold used to make the replica. Figure 2.4 shows photographs of a complete straight channel COC device and a microscopic magnified view of the microchannel. A straight channel without any defects is observed, suggesting that the micromachining procedures were successfully carried out and that microchannel had been successfully replicated in the COC device.

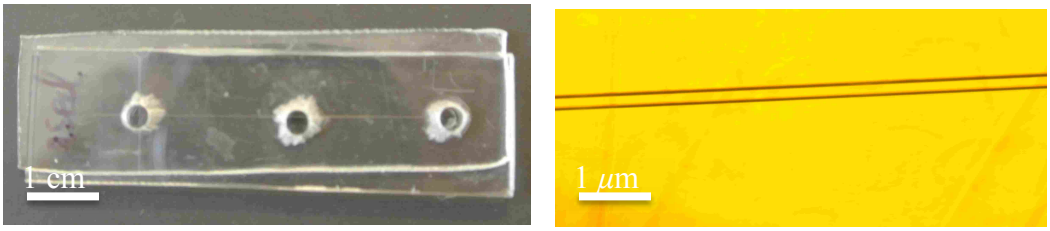

Figure 2.4 Fabricated COC device (left) and magnified view of the microchannel (right).

To further ensure that the microchannel was completely enclosed via thermal bonding and not blocked by dust or debris, 1 μL of distilled water was added to one channel reservoir and allowed to flow through the channel under pressure. If the water easily filled the channel completely, the device was considered appropriate for future testing. Otherwise, any device with difficulty filling the channel was considered defective and was discarded.

References

1. Squires, T. M.; Quake, S. R., Microfluidics: Fluid physics at the nanoliter scale. *Rev. Mod. Phys.* **2005,** *77* (3), 977-1026.
2. Janasek, D.; Franzke, J.; Manz, A., Scaling and the design of miniaturized chemical-analysis systems. *Nature* **2006,** *442* (7101), 374-80.
3. Ren, K.; Zhou, J.; Wu, H., Materials for microfluidic chip fabrication. *Acc. Chem. Res.* **2013,** *46* (11), 2396-2406.
4. Ristić, L., *Sensor technology and devices*. Artech House: 1994.
5. Harrison, D. J.; Manz, A.; Fan, Z.; Luedi, H.; Widmer, H. M., Capillary electrophoresis and sample injection systems integrated on a planar glass chip. *Anal. Chem.* **1992,** *64* (17), 1926-32.
6. Resnik, D.; Vrtacnik, D.; Mozek, M.; Pecar, B.; Amon, S., Experimental study of heat-treated thin film Ti/Pt heater and temperature sensor properties on a Si microfluidic platform. *J. Micromech. Microeng.* **2011,** *21* (2), 025025/1-025025/10.
7. Harris, N. R.; Hill, M.; Beeby, S.; Shen, Y.; White, N. M.; Hawkes, J. J.; Coakley, W. T., A silicon microfluidic ultrasonic separator. *Sens. Actuators, B* **2003,** *95* (1-3), 425-434.
8. Chen, X.; Cui, D.; Chen, J., Design, fabrication and characterization of nano-filters in silicon microfluidic channels based on mems technology. *Electrophoresis* **2009,** *30* (18), 3168-73.
9. Chartier, I.; Bory, C.; Fuchs, A.; Freida, D.; Manaresi, N.; Ruty, M.; Bablet, J.; Gilbert, K.; Sarrut, N.; Baleras, F.; Villiers, C.; Fulbert, L., Fabrication of hybrid plastic-silicon micro-fluidic devices for individual cell manipulation by dielectrophoresis. *Proc. SPIE-Int. Soc. Opt. Eng.* **2004,** *5345*, 7-16.
10. Luque, A.; Quero, J. M.; Hibert, C.; Flueckiger, P.; Ganan-Calvo, A. M., Integrable silicon microfluidic valve with pneumatic actuation. *Sens. Actuators, A* **2005,** *118* (1), 144-151.
11. Weiping, Y.; Chong, L.; Jianhua, L.; Lingzhi, M.; Defang, N., Thermal distribution microfluidic sensor based on silicon. *Sens. Actuators, B* **2005,** *108* (1-2), 943-946.
12. Nichols, K. P.; Azoz, S.; Gardeniers, H. J. G. E., Enzyme kinetics by directly imaging a porous silicon microfluidic reactor using desorption/ionization on silicon mass spectrometry. *Anal. Chem.* **2008,** *80* (21), 8314-8319.
13. Mery, E.; Ricoul, F.; Sarrut, N.; Constantin, O.; Delapierre, G.; Garin, J.; Vinet, F., A silicon microfluidic chip integrating an ordered micropillar array separation column and a nano-electrospray emitter for LC/MS analysis of peptides. *Sens. Actuators, B* **2008,** *134* (2), 438-446.
14. Baragwanath, A. J.; Swift, G. P.; Dai, D.; Gallant, A. J.; Chamberlain, J. M., Silicon based microfluidic cell for terahertz frequencies. *J. Appl. Phys.* **2010,** *108* (1), 013102/1-013102/8.
15. McMullen, J. P.; Jensen, K. F., An automated microfluidic system for online optimization in chemical synthesis. *Org. Process Res. Dev.* **2010,** *14* (5), 1169-1176.

16. Lemke, T.; Kloeker, J.; Biancuzzi, G.; Huesgen, T.; Goldschmidtboeing, F.; Woias, P., Fabrication of a normally-closed microvalve utilizing lithographically defined silicone micro o-rings. *J. Micromech. Microeng.* **2011,** *21* (2), 025011/1-025011/11.
17. Kamitani, A.; Morishita, S.; Kotaki, H.; Arscott, S., Microfabricated microfluidic fuel cells. *Sens. Actuators, B* **2011,** *154* (2), 174-180.
18. Orabona, E.; Rea, I.; Rendina, I.; De Stefano, L., A porous silicon based microfluidic array for the optical monitoring of biomolecular interactions. *Proc. SPIE* **2011,** *8073*, 807314/1-807314/6.
19. Zhang, Z. L.; MacDonald, N. C., A RIE process for submicron, silicon electromechanical structures. *J. Micromech. Microeng.* **1992,** *2* (1), 31-8.
20. Harrison D. J.; Manz, A.; Fan Z.; Ludi, H; Widmer, H. M., Capillary electrophoresis and sample injection systems integrated on a planar glass chip. *Anal. Chem.* **1992,** *64*, 1926-1932.
21. Manz, A.; Harrison, D. J.; Verpoorte, E. M.; Fettinger, J. C.; Paulus, A.; Ludi H.; Widmer, H. M., Planar chips technology for miniaturization and integration of separation technique into monitoring systems. *J. Chromatogr.* **1992,** *593*, 253-258.
22. Woolley, A. T.; Mathies, R. A., Ultra-high-speed, DNA Fragment separations using microfabricated capillary array electrophoresis chips. *Proc. Natl. Acad. Sci. U.S.A.* **1994,** *91*, 11348-11352.
23. Iliescu, C.; Taylor, H.; Avram, M.; Miao, J.; Franssila, S., A practical guide for the fabrication of microfluidic devices using glass and silicon. *Biomicrofluidics* **2012,** *6* (1), 016505, 17 pp.
24. Reschke B. R.; Schiffbauer, J.; Edwards B. F.; Timperman A. T., Simultaneous separation and detection of cations and anions on a microfluidic device with suppressed electroosmotic flow and a single injection point. *Analyst* **2010,** *135* (6), 1351-9.
25. Meagher R. J.; Thaitrong, N., Microchip electrophoresis of DNA following preconcentration at photopatterned gel membranes. *Electrophoresis* **2012,** *33* (8), 1236-41.
26. Chambers, A. G.; Ramsey, J. M., Microfluidic Dual Emitter Electrospray Ionization Source for Accurate Mass Measurements. *Anal. Chem.* **2012,** *84* (3), 1446-1451.
27. Mellors, J. S.; Gorbounov, V.; Ramsey, R. S.; Ramsey, J. M., Fully integrated glass microfluidic device for performing high-efficiency capillary electrophoresis and electrospray ionization mass spectrometry. *Anal. Chem.* **2008,** *80* (18), 6881-6887.
28. Sainiemi, L.; Sikanen, T.; Kostiainen, R., Integration of fully microfabricated, three-dimensionally sharp electrospray ionization tips with microfluidic glass chips. *Anal. Chem.* **2012,** *84* (21), 8973-8979.
29. Ahn, C. H.; Choi, J.-W., Microfluidics and their applications to lab.-on-a-chip. *Springer Handb. Nanotechnol. (2nd Ed.)* **2007**, 523-548.
30. Arora, A.; Simone, G.; Salieb-Beugelaar, G. B.; Kim, J. T.; Manz, A., Latest developments in micro total analysis systems. *Anal. Chem.* **2010,** *82* (12), 4830-4847.

31. McDonald, J. C.; Duffy, D. C.; Anderson, J. R.; Chiu, D. T.; Wu, H.; Schueller, O. J. A.; Whitesides, G. M., Fabrication of microfluidic systems in poly(dimethylsiloxane). *Electrophoresis* **2000,** *21* (1), 27-40.
32. Petersen, N. J.; Foss, S. T.; Jensen, H.; Hansen, S. H.; Skonberg, C.; Snakenborg, D.; Kutter, J. P.; Pedersen-Bjergaard, S., On-chip electro membrane extraction with online ultraviolet and mass spectrometric detection. *Anal. Chem.* **2011,** *83* (1), 44-51.
33. Jubery, T. Z.; Bottenus, D. R.; Dutta, P.; Ivory, C. F., Preconcentration of cardiac proteins in a microfluidic device. *Proc. ASME Int. Mech. Eng. Congr. Expo.--2009* **2010,** *12* (Pt. B), 613-617.
34. Reedy, C. R.; Price, C. W.; Sniegowski, J.; Ferrance, J. P.; Begley, M.; Landers, J. P., Solid phase extraction of DNA from biological samples in a post-based, high surface area poly(methyl methacrylate) (PMMA) microdevice. *Lab Chip* **2011,** *11* (9), 1603-1611.
35. Hwang, K.-Y.; Kim, J.-H.; Suh, K.-Y.; Ko, J. S.; Huh, N., Low-cost polymer microfluidic device for on-chip extraction of bacterial DNA. *Sens. Actuators, B* **2011,** *155* (1), 422-429.
36. Wang, Y.-N.; Liou, C.-L.; Wu, M.-C.; Tsai, C.-H.; Fu, L.-M., Rapid detection of methanol in an integration microfluidic chip. *Key Eng. Mater.* **2011,** *483*, 364-369.
37. Hou, H.-H.; Wang, Y.-N.; Chang, C.-L.; Yang, R.-J.; Fu, L.-M., Rapid glucose concentration detection utilizing disposable integrated microfluidic chip. *Microfluid. Nanofluid.* **2011,** *11* (4), 479-487.
38. Quist, J.; Trietsch, S. J.; Vulto, P.; Hankemeier, T., Elastomeric microvalves as tunable nanochannels for concentration polarization. *Lab Chip* **2013,** *13* (24), 4810-4815.
39. Mu, X.; Zheng, W.; Sun, J.; Zhang, W.; Jiang, X., Microfluidics for manipulating cells. *Small* **2013,** *9* (1), 9-21.
40. Khademhosseini, A.; Langer, R.; Borenstein, J.; Vacanti, J. P., Microscale technologies for tissue engineering and biology. *Proc. Natl. Acad. Sci. U. S. A.* **2006,** *103* (8), 2480-2487.
41. Ren, K.; Zare, R. N., Chemical recognition in cell-imprinted polymers. *ACS Nano* **2012,** *6* (5), 4314-4318.
42. Li, L.; Yang, Y.; Shi, X.; Wu, H.; Chen, H.; Liu, J., A microfluidic system for the study of the response of endothelial cells under pressure. *Microfluid. Nanofluid.* **2014**, DOI:10.1007/s10404-013-1275-9
43. Kayo, S.; Bahnemann, J.; Klauser, M.; Poertner, R.; Zeng, A.-P., A microfluidic device for immuno-affinity-based separation of mitochondria from cell culture. *Lab Chip* **2013,** *13* (22), 4467-4475.
44. Mukhopadhyay, R., When pdms isn't the best. *Anal. Chem.* **2007,** *79* (9), 3248-3253.
45. Shim, J. U.; Cristobal, G.; Link, D. R.; Thorsen, T.; Jia, Y.; Piattelli, K.; Fraden, S., Control and measurement of the phase behavior of aqueous solutions using microfluidics. *J. Am. Chem. Soc.* **2007,** *129* (28), 8825-8835.
46. Li, H.-F.; Lin, J.-M.; Su, R.-G.; Cai, Z. W.; Uchiyama, K., A polymeric master replication technology for mass fabrication of poly(dimethylsiloxane) microfluidic devices. *Electrophoresis* **2005,** *26* (9), 1825-1833.

47. Vazquez, M.; Paull, B., Review on recent and advanced applications of monoliths and related porous polymer gels in micro-fluidic devices. *Anal. Chim. Acta* **2010,** *668* (2), 100-113.
48. Ladner, Y.; Cretier, G.; Faure, K., Electrochromatography in cyclic olefin copolymer microchips: A step towards field portable analysis. *J. Chromatogr. A* **2010,** *1217* (51), 8001-8008.
49. Faure, K.; Albert, M.; Dugas, V.; Cretier, G.; Ferrigno, R.; Morin, P.; Rocca, J.-L., Development of an acrylate monolith in a cyclo-olefin copolymer microfluidic device for chip electrochromatography separation. *Electrophoresis* **2008,** *29* (24), 4948-4955.
50. Nge, P. N.; Pagaduan, J. V.; Yu, M.; Woolley, A. T., Microfluidic chips with reversed-phase monoliths for solid phase extraction and on-chip labeling. *J. Chromatogr. A* **2012,** *1261*, 129-135.

CHAPTER 3

PREPARATION AND OPTIMIZATION OF POROUS POLYMER MONOLITHS

3.1 Introduction

Sample preparation is crucial in quantitative bio-analysis since this is often the most time and labor intensive step in a bioanalytical method.[1, 2] In addition, sample preparation offers sample preconcentration and prevents matrix interferences in LC-MS/MS analyses.[3] Among various types of sample preparation techniques, monolithic columns have a number of advantages, *e.g.*, ease of *in-situ* preparation, controllable shape, porosity and selectivity, and fast mass transport, in an effort to overcome some of the challenges associated with other methods.

In this chapter, the preparation and optimization of an organic polymeric monolith in cyclic olefin copolymer (COC) devices fabricated as described in chapter 2 is presented. Reversed-phase porous polymer monoliths from methyl-, butyl-, octyl- and lauryl-methacrylate were synthesized and tested with pre-labeled bovine serum albumin (BSA) and myoglobin. Loading, retention and elution of pre-labeled BSA and myoglobin were measured and compared.

3.2 Experimental section

3.2.1 Materials

Cyclic olefin copolymer (Zeonor 1020R) was obtained from Zeon Chemicals (Louisville, KY). Methyl methacrylate (MMA), butyl methacrylate (BMA), octyl methacrylate (OMA), lauryl methacrylate (LMA), 2,2-dimethoxy-2-phenylacetophenone (DMPA), 1-dodecanol, ethylene dimethacrylate (EDMA), and isopropyl alcohol were purchased from Sigma–Aldrich (St. Louis, MO). Cyclohexanol was from J. T. Baker (Phillipsburg, NJ). Tween 20 was

purchased from Mallinckrodt Baker (Paris, KY). Hydroxypropyl cellulose (HPC, 100 kDa average molecular weight) was from Aldrich (Milwaukee, WI). Sodium dodecyl sulfate (SDS) was obtained from Fisher Scientific (Pittsburgh, PA). BSA and heat shock protein 90 (HSP90) were purchased from New England Biolabs (Ipswich, MA, USA). BSA was labeled with fluorescein isothiocyanate (FITC), while HSP90 was labeled with Alexa Fluor 488 TFP ester. Both fluorophores were obtained from Invitrogen (Carlsbad, CA). Anhydrous sodium carbonate, sodium bicarbonate, acetonitrile (ACN), and sodium azide were obtained from EMD Chemicals (Gibbstown, NJ), and buffer solution was prepared by mixing these four chemicals with deionized water.

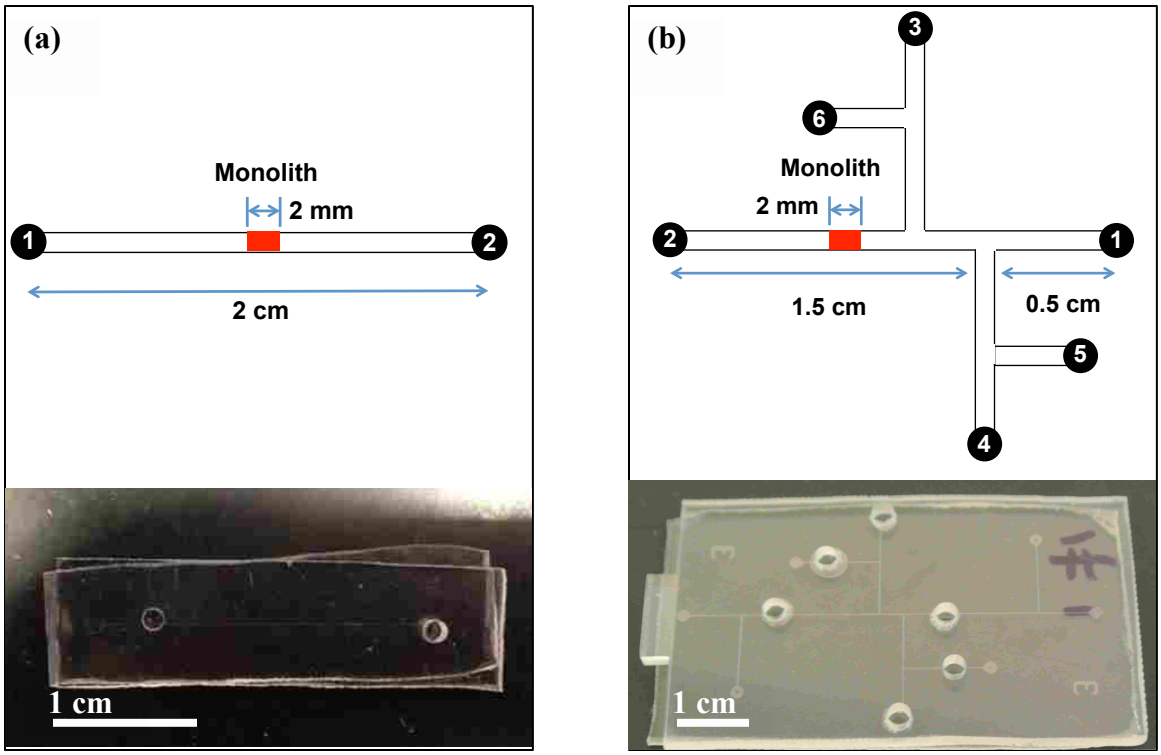

Figure 3.1 Schematic designs and photographs of microfluidic devices: (a) a single channel with two reservoirs for SPE and on-chip labeling. (b) A six-reservoir device for integrated and automated experiments, in which the reservoirs are: 1 and 2 - loading buffer, 3-elution buffer, 4-dye, 5-protein, and 6-rinsing buffer. All the channels have a width of 50 μm, and a depth of 20 μm. The monoliths are 2 mm long.

3.2.2 Device fabrication

A single COC plate was obtained by cutting a COC sheet into pieces, each having a length of 5 cm and a width of 2.5 cm with an electric motor saw. Reservoirs in the bonded device were produced by drilling holes in the cover plate. The microdevices were fabricated using a combination of photolithographic patterning, etching, hot embossing and thermal bonding as described by Kelly et al.[4] Bonding of COC was done at 110 °C for 24 min. A simple, two-reservoir layout (Figure 3.1a) was used for preliminary testing and a six-reservoir layout was used for automated and integrated SPE and on-chip labeling (Figure 3.1b). The channels in the design were approximately 50 μm wide and 20 μm deep. Channels were rinsed with isopropyl alcohol prior to polymerization of monolith.

Table 3.1 Monolith composition

Monomer (g)	Cross-linker (g)	Porogen (g)		Photoinitiator (g)	Surfactant (g per 0.5 g of mixture)
	EDMA	Cyclohexanol	1-dodecanol	DMPA	Tween 20
0.30	0.15	0.20	0.20	0.08	0.20

3.2.3 Monolith preparation in microchannels

Monoliths were fabricated by a modification of a previously reported recipe.[5] Porogens, photoinitiator, and Tween 20 were weighed according to the values listed in Table 3.1 and mixed with each different monomer (*i.e.*, MMA, BMA, OMA, or LMA). The solution was sonicated until the photoinitiator was completely dissolved and then degassed for 5 min. It was next loaded into the device, and black tape was used as a mask to expose only the desired chip region to UV radiation. Exposure was carried out with the use of a SunRay 400 lamp from Intelligent

Dispensing Systems (Encino, CA) at 200 W for 12 to 15 min. A 2 mm long monolith was formed in each microdevice in the location indicated in Figure 3.1. After polymerization, devices were rinsed with isopropyl alcohol. Then each device was washed with deionized water several times and air-dried prior to characterization and testing.

3.2.4 Characterization

Scanning electron microscopy (SEM) was carried out using a Philips XL30 ESEM FEG apparatus in low vacuum mode using a gaseous secondary detector. A voltage of 10 to 12 V was applied to the surface depending on the extent to which monolith charged. The channel with monolith was laser cut and glued on plastic stubs. The edge that contained the monolith was cut manually using a microtome with a glass knife. Once the monolith was exposed, the surface was cleaned using scotch tape to remove debris. Then the sample was mounted on aluminum stubs using carbon tape and coated with silver using a Polaron Sputterer to reduce charging during SEM imaging. The samples were coated under an applied potential of 2.5 kV, a current of 18-20 mA, and a pressure of 0.1 Torr for 3 minutes.

To evaluate the extent to which different samples adsorbed on the monolith, fluorescent dyes and two proteins (BSA and HSP90) were loaded by applying +400 V to reservoir 2 and grounding reservoir 1 for 5 min. Rinsing was done by replacing the sample in reservoir 1 with buffers having different ACN concentrations (*i.e.*, 30% and 50%) and applying the same voltages as in the previous step for 2 min. For elution, the rinse buffer in reservoir 1 was replaced with eluent consisting of 85% ACN, 15% carbonate buffer (7.5mM, pH 9.6), 0.05% HPC, and 0.05% SDS. To accomplish elution, reservoir 1 was grounded and +1000 V was applied to reservoir 2. The retention was monitored via CCD detection by measuring the background-subtracted fluorescent intensity on monoliths after rinsing and elution, to compare the retention and elution

of proteins in monoliths prepared from different monoliths. A Nikon Eclipse TE300 inverted microscope equipped with a CCD camera (Coolsnap HQ, Roper Scientific, Sarasota, FL) was used for imaging. A 488 nm blue laser (JDSU, Shenzhen, China) was used and a 10X expander was used to increase the laser beam diameter, which was directed to a 10X, 0.45 NA objective on the microscope. For fluorescence monitoring, the detection point was positioned either next to reservoir 2 (Figure 3.1), or directly on the monolith. The collected CCD images were analyzed using V++ Precision Digital Imaging software (Auckland, New Zealand).

To achieve lower detection limits, photomultiplier tube (PMT) detection was applied, in which the detection point was positioned next to reservoir 2 in Figure 3.1b. Collected fluorescence went through a D600/60 band-pass filter (Chroma, Rockingham, VT) and was detected at a Hamamatsu PMT (HC120-05, Bridgewater, NJ); out-of-focus light was blocked by a 1000 μm diameter pinhole. The PMT voltage signal was processed by a preamplifier (SR-560, Stanford Research Systems, Sunnyvale, CA) and an analog-to-digital converter (PCI 6035E, National Instruments, Austin, TX) and was recorded by LabView software running on a Dell computer.

3.2.5 Data analysis

To evaluate the extent to which proteins were retained on monoliths prepared from different monomers, 200 ng/mL of BSA was loaded on each monolith. The retention was monitored via CCD detection by measuring the background-subtracted fluorescent intensity on the monolith after rinsing and elution with 50% and 85% ACN, respectively.

3.3 Results and discussion

Thermally bonded COC devices with monoliths prepared from different monomers were prepared. COC was chosen as the substrate material because of its stability in common types of organic solvents, such as ACN used in this study for sample elution. Poly(methyl methacrylate) (PMMA) dissolves in ACN, and poly(dimethylsiloxane) (PDMS) requires additional surface modification and also swells in solvents.[6-8] Tween 20 was added as a surfactant to increase the through pore size via affecting phase separation during emulsion. Surfactant content was selected to be 30%, since monoliths prepared with higher surfactant content produced bubbles, which hindered the flow of solution in the microchannel.[9] A 70% total porogen content was selected since a soft monolith was produced when the content was above 75%, consistent with results reported by Pagaduan et al.[9]

3.3.1 Effect of monomer type

In this work, monoliths were prepared with different types of monomers (MMA, BMA, OMA, and LMA). Figure 3.2 shows SEM images of monoliths prepared with these four different monomers. For the monolith prepared from MMA (Figure 3.2a), evenly packed nodules with a diameter of approximately 500-1000 nm were observed. Through pores formed by the voids between these nodules were in the same size range. For monoliths prepared from the other three kinds of monomers, nodules with much smaller sizes were observed, which resulted in more surface area and hence more sample binding sites. For the BMA monolith (Figure 3.2b), through pores with diameters of several hundreds of nanometers were observed. A uniform monolith was observed only within the central section, while the majority of the channel contained discrete porous clusters with different lengths. This is consistent with the observations

of Ramsey and Collins,[10] which were explained by localized fluid flow during *in situ* photopolymerization. For monoliths prepared from OMA and LMA, different sizes of through pores formed by agglomerates of nodules with a diameter of approximately 100 nm were observed, which is favorable since irregular pores enhance convective transport as liquids flow through the monolith.[11]

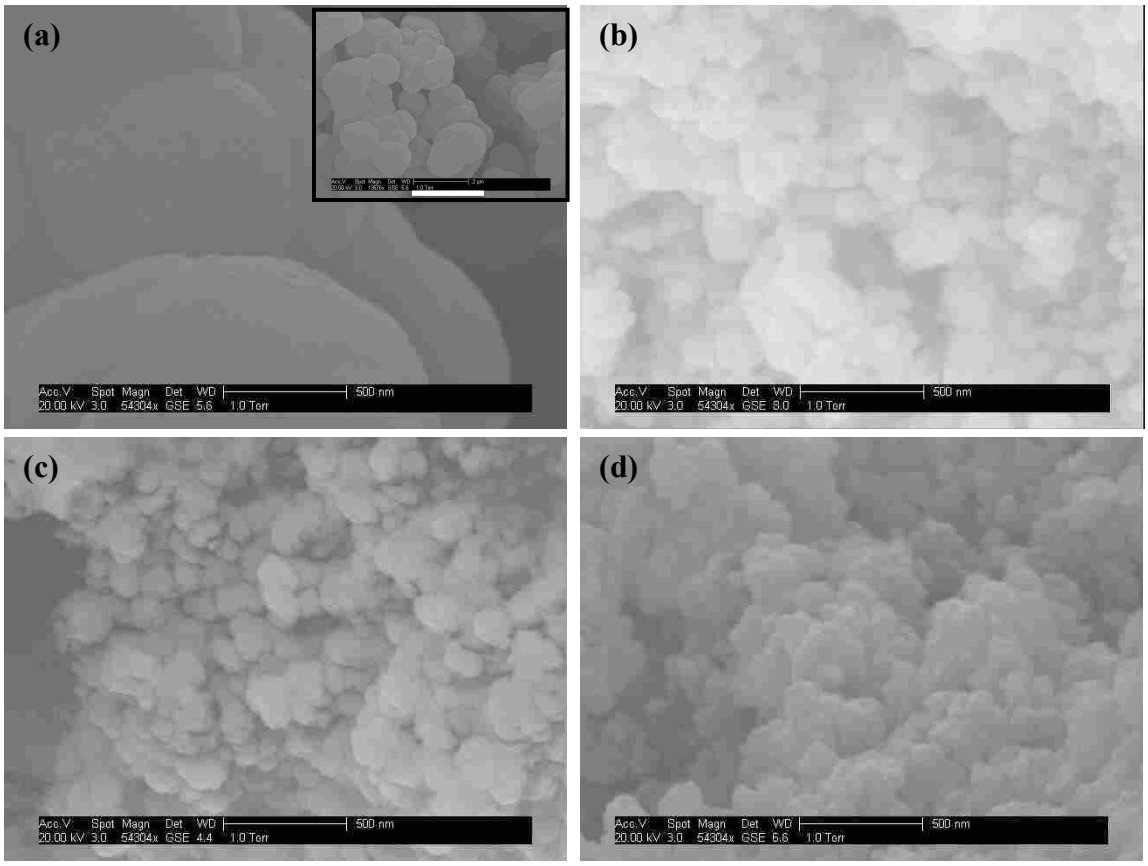

Figure 3.2 SEM images of monoliths prepared from (a) MMA (scale bar for the inset: 2 μm), (b) BMA, (c) OMA, and (d) LMA.

Figure 3.3 shows the normalized retention and elution of BSA on monoliths prepared from different monomers. First, it should be emphasized that none of the monoliths moved under the high voltage applied during rinsing and elution, in agreement with Landers et al's[12] and Nge et al's[5] results. As a result, complicated column pretreatments, such as photografting, were

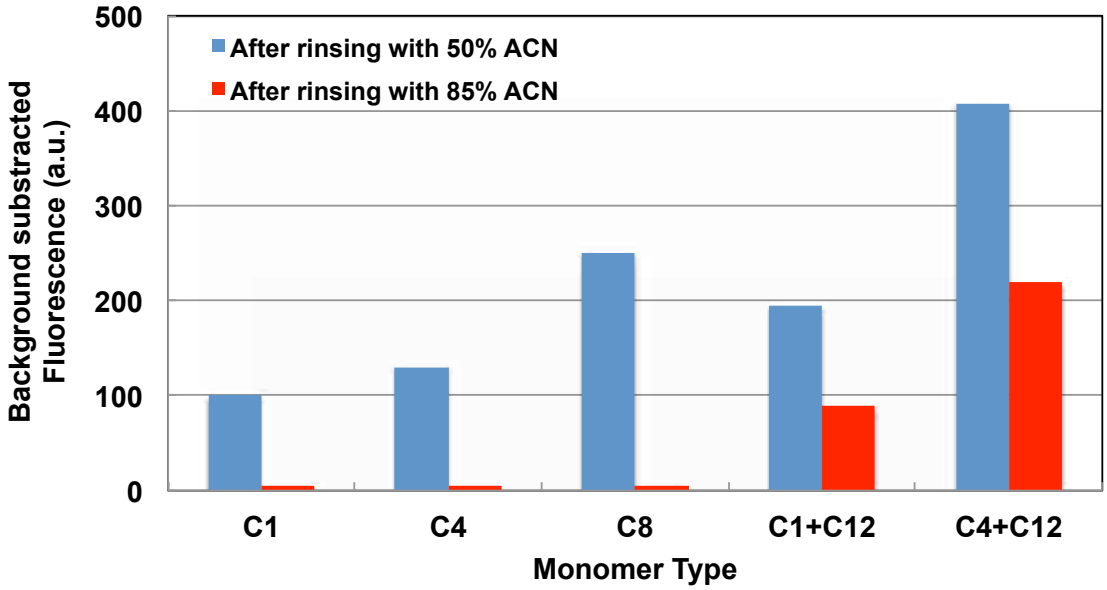

Figure 3.3 Retention and elution of BSA on monoliths prepared from different types of monomers after rinsing with 50% and 85% ACN, respectively. Measurements were done with 200 ng/mL BSA.

avoided.[12] It was observed that the retention of BSA after rinsing with 50% ACN increased for monoliths prepared from MMA, BMA, and OMA in the order of increasing carbon chain length, consistent with the increased hydrophobicity associated with the size of the monomer. Fluorescent intensities after elution with 85% ACN were very low, indicating that the retained BSA in the column was eluted almost completely. For monoliths prepared from a MMA and LMA mixture, the retention of BSA was comparable to that obtained on the one prepared from OMA, which could be explained by the introduction of MMA with lower hydrophobicity. For monoliths prepared from a BMA and LMA mixture, much higher retention was observed, which is due to the greater hydrophobicity of BMA compared to MMA. However, the fluorescent intensities for BSA on both types of mixed LMA monoliths after elution with 85% ACN remained relatively high, indicating stronger interaction between BSA and monoliths. Additionally, for monoliths prepared from LMA, buffer flow through the column was limited. In order to obtain optimal sample preconcentration, the ideal situation is high protein retention on

the monolith during rinsing, followed by complete removal during the elution step. Based on this information, monoliths prepared from OMA are the best choice.

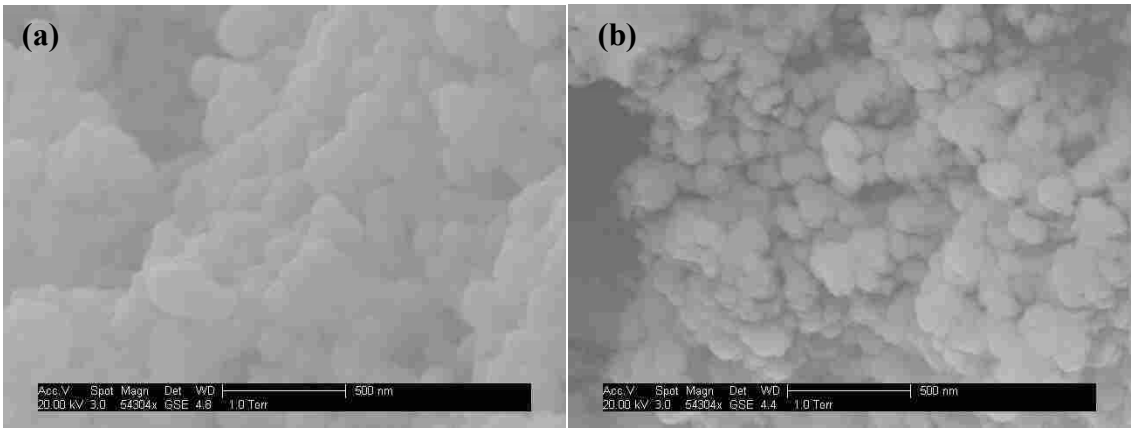

Figure 3.4 SEM images of monoliths prepared from OMA with different concentrations: (a) 20% and (b) 30%.

3.3.2 Effect of OMA concentration

Since monoliths prepared from OMA exhibit good retention and elution capabilities, their concentrations were further optimized. Figure 3.4 shows a comparison of monoliths prepared from different OMA concentrations (20% and 30%). Although the primary nodule sizes of the two monoliths were almost identical, different sizes of through pores were observed. For monoliths prepared with 20% OMA (Figure 3.4a), the observed pore diameter was approximately 500 nm, while the pore diameter for that prepared from 30% OMA was approximately 1 μm. This difference in pore size could be explained by less efficient crosslinking with the lower concentration of monomer.

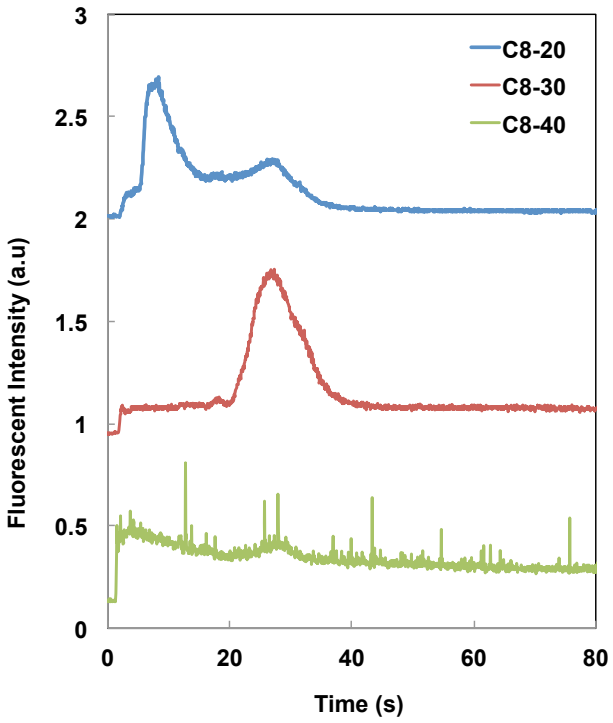

Figure 3.5 Elution of pre-labeled BSA protein with 85% ACN using monoliths prepared with different concentrations of OMA. From top to bottom: 20% OMA, 30% OMA and 40% OMA. Chromatograms are offset vertically for clarity.

Retetion results provide further insights into the optimization of these monoliths. Figure 3.5 shows a comparison of elution of pre-labeled BSA with monoliths prepared with 20%, 30%, and 40% OMA. For the monolith prepared with 20% OMA, two overlapping peaks were observed during elution. The first large peak is attributed to the fluorescent dye, while the second smaller one is assigned to labeled BSA, suggesting that not only BSA was extracted by the monolith, but also the fluorescent dye. For the monolith prepared with 40% OMA, no distinct peak of protein was observed, which could be explained by the increased interaction between protein and monolith with increased monomer content. For the monolith prepared with 30% OMA, a single peak of BSA was observed, suggesting successful extraction of BSA without retaining fluorescent dye. Therefore, an OMA monomer concentration of 30% was best suited for the extraction of proteins.

3.4 Conclusion

In summary, reversed phase polymeric monoliths in COC devices were successfully prepared and optimized. Different types and concentrations of monomers were used, and the

properties of each resultant monolith were investigated. Results show that monoliths prepared with 30% OMA were the best choice for solid phase extraction of proteins. This optimized formulation of monolith has great potential for integrating monolithic columns in microfluidic devices because of the several advantages. Monoliths formed by this optimized recipe exhibit high surface area and adjustable pore size for successful solid phase extraction. In addition, liquid solution, such as buffer solutions, can flow through the optimized monolith by capillary action, and electrophoretic flow can be used to move fluid through the monolith.

References

1. Cabrera, K., Applications of silica-based monolithic hplc columns. *J. Sep. Sci.* **2004,** *27* (10-11), 843-852.
2. Xiong, L.; Zhang, R.; Regnier, F. E., Potential of silica monolithic columns in peptide separations. *J. Chromatogr. A* **2004,** *1030* (1-2), 187-194.
3. Skudas, R.; Grimes, B. A.; Machtejevas, E.; Kudirkaite, V.; Kornysova, O.; Hennessy, T. P.; Lubda, D.; Unger, K. K., Impact of pore structural parameters on column performance and resolution of reversed-phase monolithic silica columns for peptides and proteins. *J. Chromatogr. A* **2007,** *1144* (1), 72-84.
4. Kelly, R. T.; Woolley, A. T., Thermal bonding of polymeric capillary electrophoresis microdevices in water. *Anal. Chem.* **2003,** *75* (8), 1941-1945.
5. Nge, P. N.; Pagaduan, J. V.; Yu, M.; Woolley, A. T., Microfluidic chips with reversed-phase monoliths for solid phase extraction and on-chip labeling. *J. Chromatogr. A* **2012,** *1261*, 129-135.
6. Ren, K.; Zhou, J.; Wu, H., Materials for microfluidic chip fabrication. *Acc. Chem. Res.* **2013,** *46* (11), 2396-2406.
7. Ahn, C. H.; Choi, J.-W., Microfluidics and their applications to lab.-on-a-chip. *Springer Handb. Nanotechnol. (2nd Ed.)* **2007**, 523-548.
8. Le Gac, S.; Carlier, J.; Camart, J.-C.; Cren-Olive, C.; Rolando, C., Monoliths for microfluidic devices in proteomics. *J Chromatogr B* **2004,** *808* (1), 3-14.
9. Pagaduan, J. V.; Yang, W.; Woolley, A. T., Optimization of monolithic columns for microfluidic devices. *Proc. SPIE* **2011,** *8031*, 80311V/1-80311V/7.
10. Ramsey, J. D.; Collins, G. E., Integrated microfluidic device for solid-phase extraction coupled to micellar electrokinetic chromatography separation. *Anal. Chem.* **2005,** *77* (20), 6664-6670.
11. Svec, F., Organic polymer monoliths as stationary phases for capillary HPLC. *J. Sep. Sci.* **2004,** *27* (17-18), 1419-1430.
12. Ladner, Y.; Cretier, G.; Faure, K., Electrochromatography in cyclic olefin copolymer microchips: A step towards field portable analysis. *J. Chromatogr. A* **2010,** *1217* (51), 8001-8008.

CHAPTER 4

MONOLITHIC SOLID PHASE EXTRACTION IN MICROFLUIDICS

4.1 Introduction

With the monolith composition optimization finished, the next step in device development is to demonstrate the solid phase extraction (SPE) function of the monolith. To do this, the retention and elution of two prelabeled proteins, heat shock protein 90 (HSP90) and bovine serum albumin (BSA), were tested first. Then on-chip labeling of HSP90 with the fluorescent dye Alexa Fluor 488 TFP ester was tested. Finally, automated integrated SPE and on-chip labeling of HSP90 were performed.

4.2 Experimental section

The microdevices were fabricated using a combination of photolithographic patterning, etching, hot embossing and thermal bonding as described in Section 2.2. The two device layouts are shown in Figure 3.1. Monolith fabrication is described in Section 3.2.3.

4.2.1 Instrumentation and microdevice operation

Off-chip labeling of HSP90 with Alexa Fluor TFP 488 ester was done using a process similar to the one described by Nge et al.[1] Briefly, HSP90 solution was prepared in bicarbonate buffer at a concentration of 220 μg/mL. Alexa Fluor 488 TFP ester solution (5 μL) with a concentration of 10 mg/mL in dimethyl sulfoxide (DMSO) was added to 250 μL of protein solution and incubated in the dark overnight at room temperature. Unconjugated dye was filtered

from the protein using an Eppendorf 5418 centrifugal filter device. The labeled protein samples were collected and then stored in the dark at 4 °C until used.

Before sample loading, monolithic columns were rinsed with 2-propanol several times to clean the channel surface, and then bicarbonate buffer (10 mM, pH 9.3) was vacuumed into the channel. Next, the stability of the current was examined by applying +600 V to reservoir 2 and grounding reservoir 1 for 1 min (see Figure 3.1 for reservoir numbering). At the same time, the microdevice was observed in a Nikon Eclipse TE300 inverted microscope coupled with CCD camera (Coolsnap HQ, Roper Scientific, Sarasota, FL) to make sure no bubbles were trapped in the microchannel.

After column preconditioning and prescreening, operation for the simple design (Figure 3.1a) was as follows. For SPE experiments, labeled protein samples were placed in reservoir 1 and loaded by applying +600 V to reservoir 2 and grounding reservoir 1 for 10 min. A 200 μg/mL solution of labeled HSP90 was loaded onto a column with a in-situ grown OMA monolith, and a control was done by loading the same sample into a column without monolith. Both columns were eluted by placing 85% ACN in reservior 1 and applying the same voltages as in the loading step.

To evaluate the extent to which different samples adsorbed on the monolith, on column imaging was performed to measure background-subtracted fluorescence intensities after the rinsing and elution steps. Fluorescent dyes, fluorescein isothiocyanate (FITC) and Alexa Fluor 488 TFP ester, (each 100 nM) and proteins (BSA and HSP90) were transferred into reservoir 1 and loaded by applying +400 V to reservoir 2 and grounding reservoir 1 for 5 min. Rinsing and elution were done by replacing the sample in reservoir 1 with 50% and 85% ACN, respectively. In these two steps, +600 V were applied to reservoir 2 and reservoir 1 was grounded.

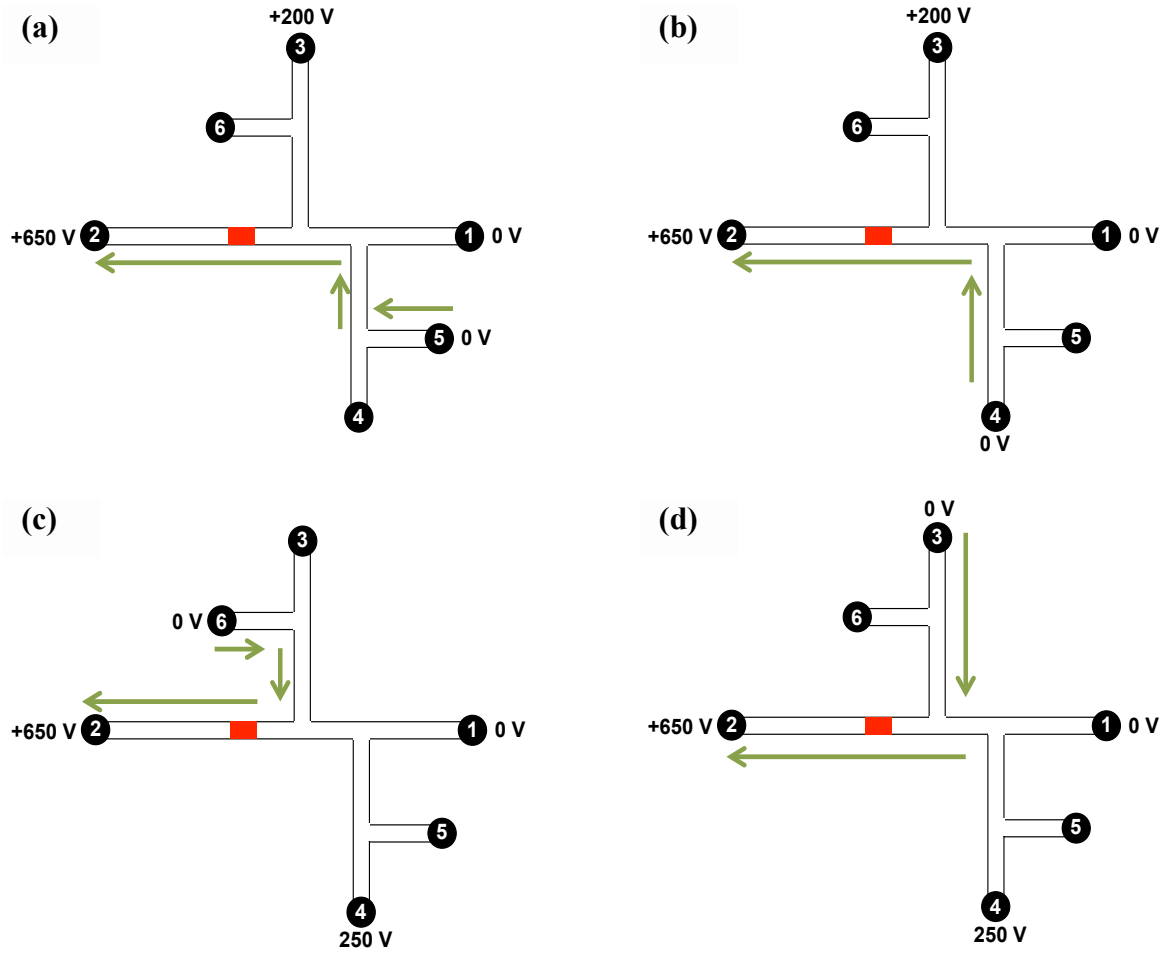

Figure 4.1 Schematic of automated device operation: (a) loading, (b) labeling, (c) rinsing, and (d) elution. Reservoirs 1 and 2 were filled with bicarbonate buffer, and reservoirs 3 to 6 were filled with elution solution (85% ACN and 15% bicarbonate buffer), dye, HSP90, and rinsing solution (50% ACN and 50% bicarbonate buffer), respectively. (a) For sample loading, reservoirs 1 and 5 were grounded, and +650 V and +200 V were applied to reservoirs 2 and 3, respectively. (b) For sample labeling, reservoirs 1 and 4 were grounded, and +650 V and +200 V were applied to reservoirs 2 and 3, respectively. (c) For rinsing, reservoirs 1 and 6 were grounded, and +650 V and +250 V were applied to reservoirs 2 and 4, respectively. (d) For elution, reservoirs 1 and 3 were grounded, and +650 V and +250 V were applied to reservoirs 2 and 4, respectively. The solution flow directions are indicated by arrows.

For on-chip labeling experiment in the simple device (Figure 3.1a), unlabeled protein samples were loaded in the same way as the labeled samples. Next, reservoir 1 was rinsed and filled with fluorescent dye solution (10 mg/mL) in DMSO. This solution was driven through the column by applying the same voltages as in loading for 10 min, followed by incubation for 10-15 min with the voltage off. Rinsing was performed by replacing the labeling solution in reservoir 1

with buffer having different ACN concentrations (*i.e.*, 30% and 50%) and applying the same voltages as in the previous step for 10 min. For elution, the rinse solution in reservoir 1 was replaced with eluent consisting of 85% ACN and 15% bicarbonate buffer. During elution, reservoir 1 was grounded while a voltage of +600 V was applied to reservoir 2 for 10 min.

For integrated automation experiments conducted on microdevices based on the design in Figure 3.1b, platinum wires were inserted into the solution-filled reservoirs to provide electrical contact. Two high-voltage power supplies provided all applied potentials. A custom-designed voltage-switching box was controlled by LabView and applied potentials to the microchips. Reservoirs 1 and 2 were filled with bicarbonate buffer, and reservoirs 3 to 6 were filled with elution solution (85% ACN and 15% bicarbonate buffer), dye, HSP90 (20 nM), and rinsing solution (50% ACN and 50% bicarbonate buffer), respectively. Automated experiments were performed through the steps shown in Figure 4.1. In each step, voltages were applied to different reservoirs for 10 min as listed in Table 4.1. The CCD and PMT detection setup was the same as described in Section 3.2.4.

Table 4.1 Voltages applied to reservoirs for each step in automation experiments

Reservoir	1	2	3	4	5	6
Loading	0	650	200	-	0	-
Labeling	0	650	200	0	-	-
Rinsing	0	650	-	250	-	0
Elution	0	650	0	250	-	-

"0" indicate the reservoir is grounded and "-" indicate the reservoir is floated

4.3 Results and discussion

4.3.1 Solid phase extraction and preconcentration of proteins on OMA monoliths

As shown in Figure 4.2, different elution profiles of HSP90 were observed for columns with and without a monolith. For elution of HSP90 without a monolith, several peaks were

observed. The first two sharp peaks were assigned to unconjugated dye, and the third, small peak at a retention time of approximately 18 seconds was attributed to HSP90. In contrast, for elution from an OMA monolith, a single peak was observed at a retention time of approximately 22 seconds. For protein sample in both conditions, the retention time of HSP90 was similar, but the peak area of the monolith extracted sample was approximately fourfold larger. The small peak area observed from elution without monolith was attributed to residual HSP90 after rinsing the reservoir, while the larger peak area observed from elution from the OMA monolith confirmed successful protein enrichment.

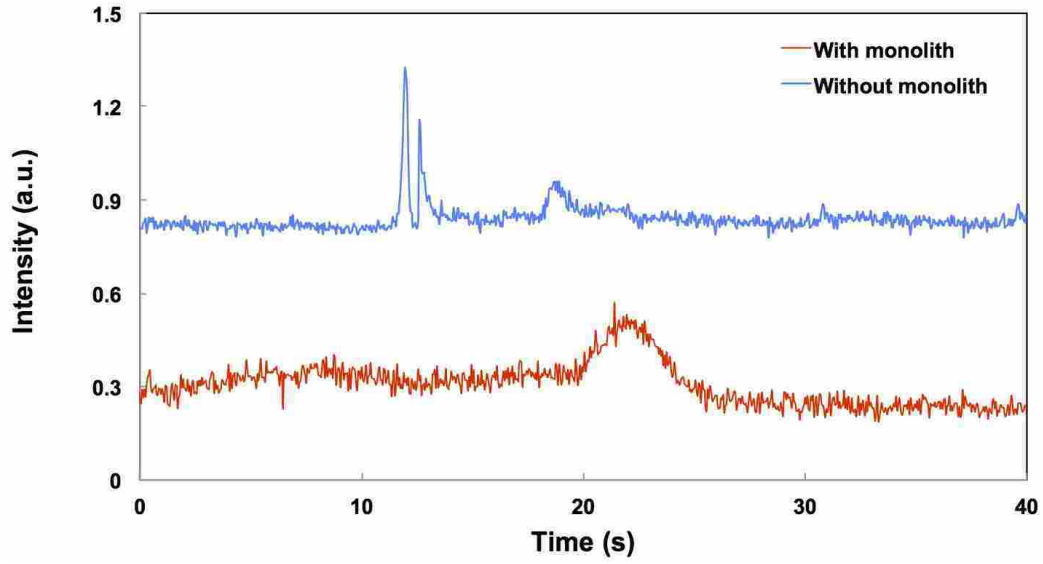

Figure 4.2 Voltage driven elution profile of labeled HSP90 in a column with and without monolith. Traces are offset vertically for clarity.

4.3.2 Retention of sample on OMA monoliths

Figure 4.3 shows the normalized retention of fluorescent dyes and proteins on OMA monoliths. Retention of the fluorescent dyes (Alexa Fluor 488 ester and FITC) on the column was relatively low, while retention of proteins (HSP90 and BSA) on the OMA monolith was clearly higher, which is consistent with the results reported by Nge et al.[2]

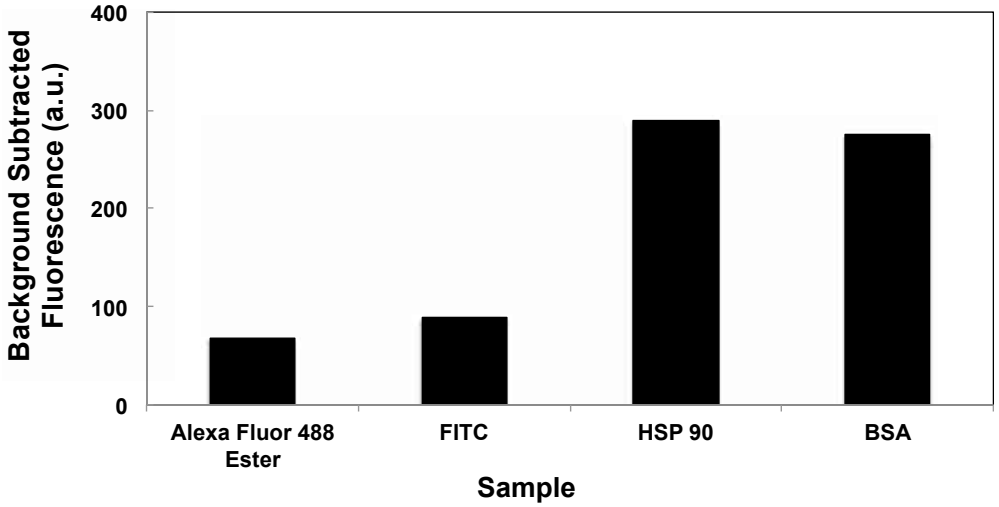

Figure 4.3 Retention of dyes and proteins.

Previous studies showed that preconditioning of monolithic columns influences the retention of amino acids and proteins.[3] Nge et al.[2] showed that the greatest retention of protein was observed when a BMA monolith was rinsed with 30% ACN just before sample loading, which was reported to help remove impurities and activate and/or hydrate the monolith surface to provide adequate contact with the liquid sample.[4] However, good retention of protein on OMA monoliths was observed without preconditioning with ACN, which may be explained by the difference in hydrophobicity between BMA and OMA monoliths.

4.3.3 Elution of samples from OMA monoliths

Figure 4.4 shows 85% ACN elution profiles of labeled proteins and their corresponding fluorescent dyes on an OMA column that had already been rinsed with 50% ACN. For the elution of HSP90 and Alexa Fluor 488 TFP ester (Figure 4.4a), a single peak of HSP90 was seen at approximately 20 seconds, while no peak for Alexa Fluor 488 TFP ester was observed, presumably because the rinse step eluted all the dye. This result showed that labeled HSP90 was adsorbed and retained on the monolith after rinsing with 50% ACN solution and successfully

eluted using 85% ACN, while Alexa Fluor 488 TFP ester was rinsed off with 50% ACN, consistent with their retention on the monolith shown in Figure 4.3. In a different experiment done under the same conditions, a single peak of labeled BSA was eluted with 85% ACN, while no peak for FITC was observed in the 85% ACN elution after a 50% ACN rinse (Figure 4.4b), suggesting successful retention and elution of BSA on an OMA monolith.

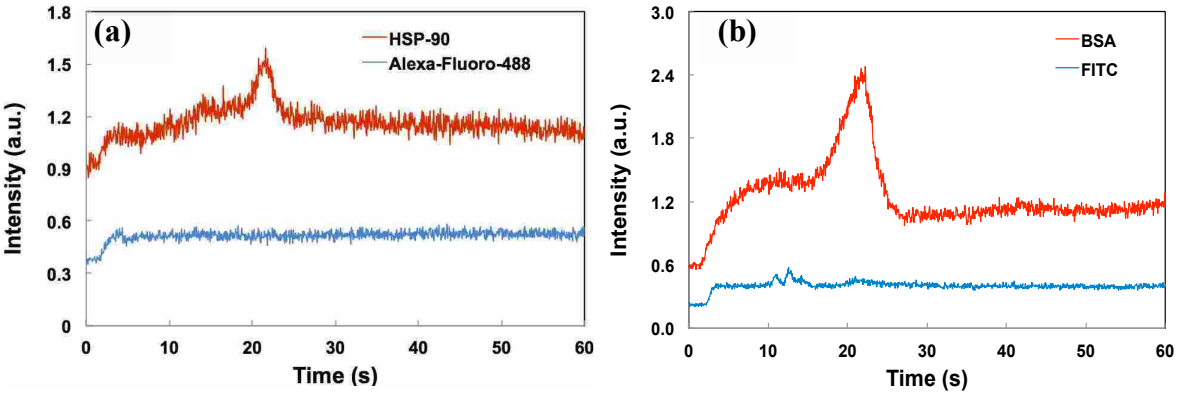

Figure 4.4 Elution profiles of labeled protein and fluorescent dye from OMA monolithic columns. (a) HSP90 and Alexa Fluor 488 TFP ester and (b) BSA and FITC. Traces are offset vertically for clarity.

In addition, different concentrations of labeled BSA were eluted using an OMA column. In the elution profiles of BSA, peak areas increased with BSA concentration (Figure 4.5a). The plot of peak area versus BSA concentration (Figure 4.5b) showed very poor correlation between peak area and concentration. Indeed, a 100-fold increase in BSA concentration increased the peak area by less than four fold, demonstrating less than ideal potential for quantitative work with these initial results. This may be due to the limited retention capacity of the monolith: the active binding sites on the monolith may be saturated by the higher concentrations of BSA, such that not all the BSA was retained on the monolith.

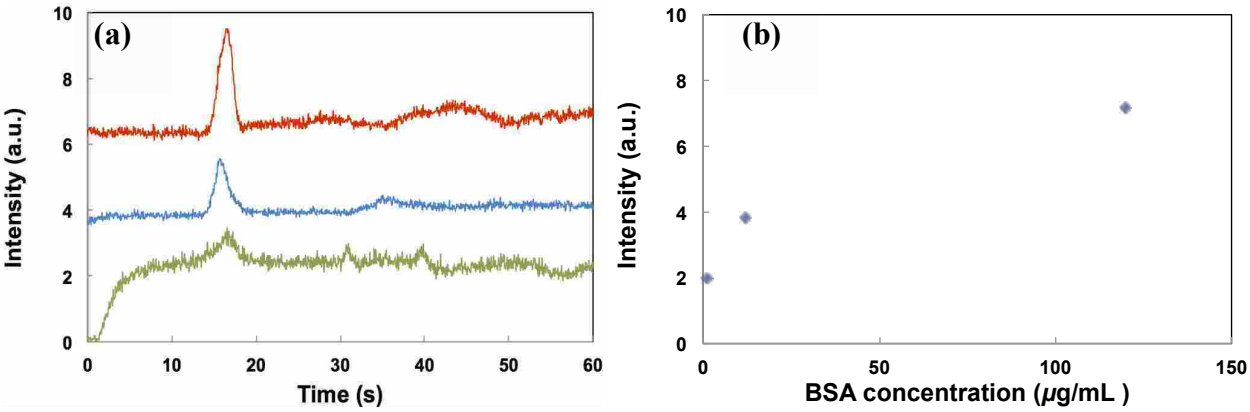

Figure 4.5 Elution of labeled BSA using an OMA monolithic column. (a) Elution of BSA of different concentrations (bottom: 1.2 μg/mL, middle: 12 μg/mL, and top: 120 μg/mL). Traces are offset vertically for clarity. (b) Plot of peak area as a function of BSA concentration.

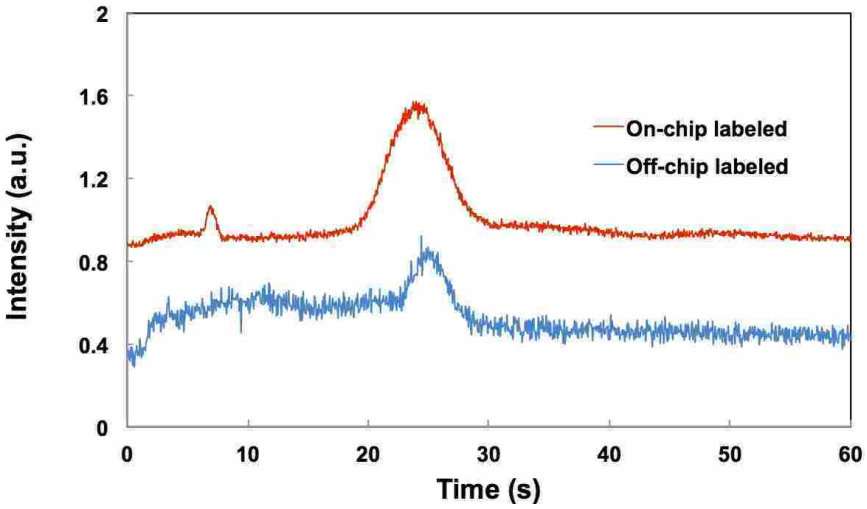

Figure 4.6 Elution profiles of HSP90 labeled on-chip and off-chip. Traces are offset vertically for clarity.

4.3.4 Off- and on-chip labeling of HSP90 with Alexa Fluor 488 TFP ester

Figure 4.6 shows elution profiles for HSP90 labeled off- and on-chip with Alexa Fluor 488 TFP ester. It was observed that the elution of HSP90 labeled on-chip with Alexa Fluor 488 ester was similar to that for protein labeled off-chip. Protein peaks in both samples appeared at approximately the same time (~25 s). The small peak at approximately 8 seconds was observed

in the on-chip labeled sample, which is attributed to unconjugated fluorescent dye due to the shorter incubation time (15 min for on-chip labeling versus overnight for off-chip labeling). This result shows that on-chip labeling can be integrated with automated SPE in a single microfluidic device.

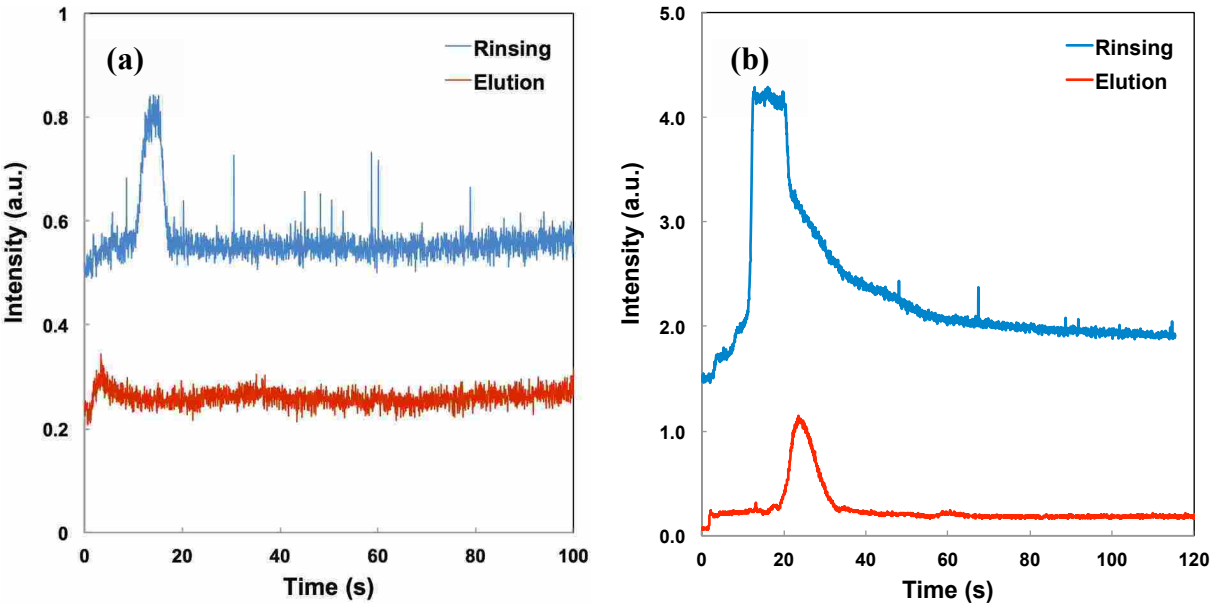

Figure 4.7 Rinsing and elution profiles of (a) pure Alexa Fluor 488 TFP ester and (b) HSP90 in automation. Traces are offset vertically for clarity.

4.3.5 Automated analysis of samples

To test the feasibility of automated and integrated on-chip SPE, preconcentration, and on-chip labeling, a six-reservoir microchip with OMA monolith in the microchannel (Figure 3.1b) was used. Automated loading and elution of 10 mg/mL Alexa Fluor 488 TFP ester, as well as on-chip labeling HSP90 were carried out separately, and the results are shown in Figure 4.7. For the Alexa Fluor 488 TFP ester solution, a single peak at around 17 seconds was observed in the rinsing step with 50% ACN, while no obvious peak was observed in elution with 85% ACN (Figure 4.7a), indicating that essentially all of the dye was eluted from the monolith in the rinsing

step. For on-chip labeling HSP90 (Figure 4.7b), a peak at around 20 seconds was observed in the rinsing step, similar to that observed in the rinsing of the Alexa Fluor 488 TFP ester solution. In the elution step, a single peak at approximately 24 seconds was observed, indicating that HSP90 was successfully extracted, labeled, and eluted on-chip in an automated manner.

4.4 Conclusion

In this chapter, the optimized OMA monolith was applied as a solid support for on-chip labeling. Successful sample extraction and on-chip labeling were shown. HSP90 and BSA samples were retained and eluted through SPE on an OMA monolith in a microfluidic device. In addition, HSP90 was fluorescently labeled on-chip, while the unreacted dye was eluted separately from the labeled protein. Conditions for automated on-chip fluorescent labeling of protein were developed.

The combination of the proven enrichment capacity of SPE with on-chip labeling shows great potential to address the need for sample pretreatment and preconcentration. In addition, this approach can be further integrated with other sample pretreatment techniques, such as affinity extraction, to achieve greater specificity, providing powerful and automated approaches for more complicated bioanalysis.

References

1. Nge, P. N.; Yang, W.; Pagaduan, J. V.; Woolley, A. T., Ion-permeable membrane for on-chip preconcentration and separation of cancer marker proteins. *Electrophoresis* **2011,** *32* (10), 1133-1140.
2. Nge, P. N.; Pagaduan, J. V.; Yu, M.; Woolley, A. T., Microfluidic chips with reversed-phase monoliths for solid phase extraction and on-chip labeling. *J. Chromatogr. A* **2012,** *1261*, 129-135.
3. Augustin, V.; Jardy, A.; Gareil, P.; Hennion, M.-C., In situ synthesis of monolithic stationary phases for electrochromatographic separations: Study of polymerization conditions. *J. Chromatogr. A* **2006,** *1119* (1-2), 80-87.
4. Marchiarullo, D. J. Development of microfluidic technologies for on-site clinical and forensic analysis: Extraction, amplification, separation, and detection, Dissertation, University of Virginia, 2009.

CHAPTER 5

CONCLUSIONS AND FUTURE WORK

5.1 Conclusions

5.1.1 Optimized monoliths for solid phase extraction

Reversed phase, polymeric monoliths in cyclic olefin copolymer (COC) devices in Chapter 3 were successfully prepared and optimized. Different types and concentrations of monomers were used, and each resultant monolith was characterized. Retention experiments on proteins were conducted to evaluate monolith performance. Results show that monoliths prepared with 30% octyl methacrylate (OMA) were the best choice for solid phase extraction (SPE) of selected proteins.

This optimized formulation of monolith offers advantages. These monoliths exhibit high surface area and adjustable pore size for successful SPE. HSP90 and BSA were successfully extracted and eluted. Furthermore, liquid solutions, such as aqueous buffers and solvents like acetonitrile, flow through the optimized monolith by capillary action. Finally, electrophoretic methods can be used to move fluid through the column, avoiding the use of equipment to generate high pressure and offering potential for further integration.

5.1.2 On-chip labeling and automation

Monoliths optimized in Chapter 3 were prepared in microchannels in COC devices. A comparison between the elution profiles of off-chip labeled HSP90 with and without the monolith demonstrated successful sample enrichment and improved peak specificity.

Subsequently, monolithic SPE with on-chip labeling was integrated. HSP90 was fluorescently labeled on chip, while unreacted dye was eluted separately from the labeled protein. Results showed that HSP90 was labeled with Alexa Fluor 488 TFP ester in 15 minutes. Finally, automated conditions for integrated on-chip SPE and labeling were tested and evaluated.

The combination of SPE and on-chip labeling showed potential to address the need for sample preconcentration and pretreatment. The ease of monolith preparation and fast on-chip labeling could reduce analysis time and effort compared other techniques. In addition, this approach can be further integrated with other sample preparation and separation techniques to achieve greater specificity for more complicated bioanalysis.

5.2 Future work

5.2.1 Optimization of monoliths

Although experiments were able to demonstrate proof-of-concept with SPE using polymeric monoliths, quantification of protein biomarkers still requires more work. As shown in Chapter 4, the relationship between different HSP90 concentrations and their corresponding peak area in the elution profiles did not follow the expected linear trend, which may be due in part to the retention capacity of these monoliths.

There are several device parameters can be further modified to achieve better quantification capability. First, the ratio of monomer to porogen can be further adjusted to change the column porosity, which influences the surface area, column flow rate, and the resultant retention and elution. In addition, experimental conditions, such as the highest voltages that can be applied without solvent evaporation due to Joule heating, are also affected by surface area and porosity, which in turn determines the peak shape and capacity. Moreover, column length can be tuned to

vary loading capacity. With these conditions optimized, quantitative experiments can be conducted, and corresponding calibration methods can be established.

5.2.2 Integration

Future challenges in liquid based separation techniques are in life science applications, especially for screening and analysis of biomarkers for diagnosis. Although biomarker analysis has been demonstrated in microfluidics, detection and quantification for real samples remains preliminary. Biofluids in human, animals and plants are extremely complex, consisting of a variety of substances with different compositions and structures. Therefore, better selectivity, higher sensitivity, and lower detection limits are important in bioanalysis. These problems can be addressed through multidimensional combination of extraction, separation, and detection in microfluidic systems.

Potential for integration of multiple functions in a single, miniaturized device has been a central advantage of microfluidics. Microfluidic devices integrating sample extraction, purification, preconcentration, separation and detection offer great potential for point of care applications. Microfluidic systems integrating monolithic columns have been used for SPE, preconcentration, mixing, and separation, as summarized by several in-depth reviews.[1, 2]

The monoliths reported in this work have potential to be integrated with upstream immunoaffinity sample extraction and downstream electrophoresis separation. The Woolley group has demonstrated the integration of immunoaffinity extraction and electrophoresis separation for cancer-relevant samples in blood serum.[3, 4] In fact, a design for integration, as shown in Figure 5.1, has been proposed. Biofluid is loaded in the device and first passes through the affinity column, in which target biomarkers are extracted via antibody-antigen interaction. Subsequently, the extracted biomarkers are released and pass through the enrichment column for

preconcentration and fluorescence labeling. Finally, labeled biomarkers are eluted, and then separated by electrophoresis.

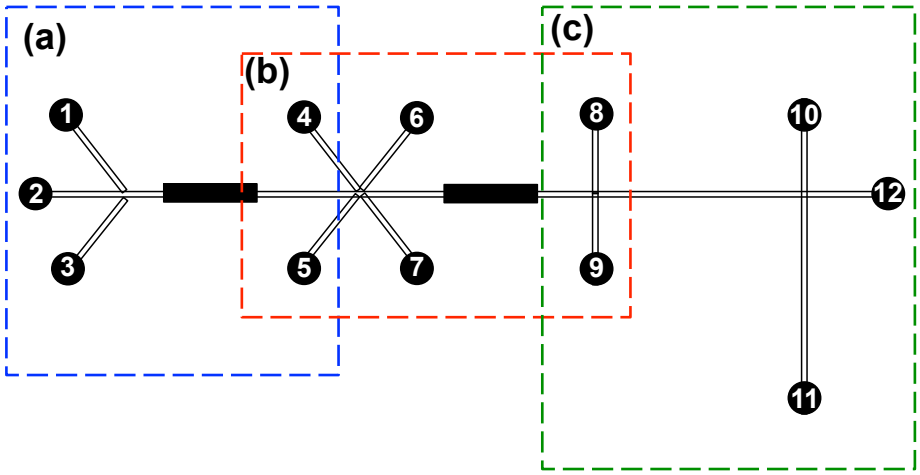

Figure 5.1 Layout of the proposed integration of (a) immunoaffinity extraction (blue), (b) sample preconcentration and labeling (red), and (c) electrophoresis separation (green). The affinity column is the black filled rectangle on the left, and the enrichment column is the black filled rectangle near the middle. Reservoirs numbering is: 1-sample, 2-wash, 3-affinity eluent, 4-affinity waste, 5-fluorescence label, 6-label eluent, 7-protein eluent, 8-elution waste, 9-microchip electrophoresis injection, 10-electrophoresis buffer, 11-electrophoresis waste, and 12-injection waste.

5.3 Outlook

In summary, in my thesis I have developed a monolithic column integrated with sample preconcentration and on-chip labeling. Further integration of this monolithic column with other microfluidic components should provide additional selectivity, along with separation and detection. This thus contributes to the development of integration and miniaturization. Combined with rapid developments in other areas, such as novel materials, fabrication and engineering techniques, microfluidics will have a profound impact on the future of life sciences.

References

1. Svec, F., Less common applications of monoliths: Preconcentration and solid-phase extraction. *J Chromatogr B,* **2006,** *841* (1-2), 52-64.
2. Vazquez, M.; Paull, B., Review on recent and advanced applications of monoliths and related porous polymer gels in micro-fluidic devices. *Anal. Chim. Acta* **2010,** *668* (2), 100-113.
3. Yang, W.; Yu, M.; Sun, X.; Woolley, A. T., Microdevices integrating affinity columns and capillary electrophoresis for multibiomarker analysis in human serum. *Lab Chip* **2010,** *10* (19), 2527-2533.
4. Yang, W.; Sun, X.; Wang, H.-Y.; Woolley A. T., Integrated microfluidic device for serum biomarker quantitation using either standard addition or a calibration curve. *Anal Chem* **2009,** *81* (19), 8230-5.